

Published in final edited form as:

*J Phys Chem A*. 2008 August 21; 112(33): 7723–7733. doi:10.1021/jp8043626.

## Effects of Structural Deformations on Optical Properties of Tetrabenzoporphyrins: Free-Bases and Pd Complexes

 Artem Y. Lebedev<sup>†</sup>, Mikhail A. Filatov<sup>‡</sup>, Andrei V. Cheprakov<sup>‡, \*</sup>, and Sergei A. Vinogradov<sup>†, \*</sup>
<sup>†</sup>*Department of Biochemistry and Biophysics, UniVersity of Pennsylvania, Philadelphia, Pennsylvania 19104*
<sup>‡</sup>*Department of Chemistry, Moscow State UniVersity, Moscow 119899, Russia*

### Abstract

A recently developed method of synthesis of  $\pi$ -extended porphyrins made it possible to prepare a series of tetrabenzoporphyrins (TBP) with different numbers of *meso*-aryl substituents. The photophysical parameters of free-bases and Pd complexes of *meso*-unsubstituted TBP's, 5,15-diaryl-TBP's ( $\text{Ar}_2\text{TBP}$ 's) and 5,10,15,20-tetraaryl-TBP's ( $\text{Ar}_4\text{TBP}$ 's) were measured. For comparison, similarly *meso*-arylsubstituted porphyrins fused with nonaromatic cyclohexeno-rings, i.e.  $\text{Ar}_n$ -tetracyclohexenoporphyrins ( $\text{Ar}_n\text{TCHP}$ 's,  $n = 0, 2, 4$ ), were also synthesized and studied. Structural information was obtained by ab initio (DFT) calculations and X-ray crystallography. It was found that: 1) Free-base  $\text{Ar}_4\text{TBP}$ 's are strongly distorted out-of-plane (saddled), possess broadened, red-shifted spectra, short excited-state lifetimes and low fluorescence quantum yields ( $\tau_{\text{fl}} = 2\text{--}3$  ns,  $\phi_{\text{fl}} = 0.02\text{--}0.03$ ). These features are characteristic of other nonplanar free-base porphyrins, including  $\text{Ar}_4\text{TCHP}$ 's. 2)  $\text{Ar}_2\text{TBP}$  free-bases possess completely planar geometries, although with significant in-plane deformations. These deformations have practically no effect on the singlet excited-state properties of  $\text{Ar}_2\text{TBP}$ 's as compared to planar *meso*-unsubstituted TBP's. Both types of porphyrins retain strong fluorescence ( $\tau_{\text{fl}} = 10\text{--}12$  ns,  $\phi_{\text{fl}} = 0.3\text{--}0.4$ ), and their radiative rate constants ( $k_{\text{r}}$ ) are 3–4 times higher than those of planar  $\text{H}_2\text{TCHP}$ 's. 3) Nonplanar deformations dramatically enhance nonradiative decay of triplet states of regular Pd porphyrins. For example, planar PdTCHP phosphoresces with high quantum yield ( $\phi_{\text{phos}} = 0.45$ ,  $\tau_{\text{phos}} = 1118$   $\mu\text{s}$ ), while saddled PdPh<sub>4</sub>TCHP is practically nonemissive. In contrast, both ruffled and saddled PdAr<sub>n</sub>TBP's retain strong phosphorescence at ambient temperatures (PdPh<sub>2</sub>TBP:  $\tau_{\text{phos}} = 496$   $\mu\text{s}$ ,  $\phi_{\text{phos}} = 0.15$ ; PdPh<sub>4</sub>TBP:  $\tau_{\text{phos}} = 258$   $\mu\text{s}$ ,  $\phi_{\text{phos}} = 0.08$ ). It appears that  $\pi$ -extension is capable of counterbalancing deleterious effects of nonplanar deformations on triplet emissivity of Pd porphyrins.

### Introduction

Porphyrins extended by way of annealing the pyrrole residues with external aromatic rings are commonly referred to as  $\pi$ -extended porphyrins. Symmetrically  $\pi$ -extended porphyrins, e.g., tetrabenzoporphyrins and tetranaphthoporphyrins, possess high absorption in the near-infrared region of the spectrum, and consequently draw attention in photomedicine,<sup>1</sup> biomedical sensing and imaging.<sup>2</sup> In addition,  $\pi$ -extended porphyrins have shown promise in up-conversion of noncoherent infrared light,<sup>3</sup> optical power limiting and electrooptical applications<sup>4</sup> as well as in material science.<sup>5</sup> Such broad range of applicability warrants in-depth studies of structure–property relationships in the family of  $\pi$ -extended porphyrins, especially in the area of their photophysics, which is central to many of their applications.

\*To whom correspondence should be addressed. E-mail: E-mail: vinograd@mail.med.upenn.edu (S.A.V.); E-mail: avchep@elorg.chem.msu.ru (A.V.C.).

Starting 1960s, influence of the  $\pi$ -extension on optical properties of porphyrins has been addressed by a number of researchers.<sup>6–8</sup> As early as in 1961, Gouterman applied his four-orbital model to qualitatively explain differences between the electronic absorption spectra of regular porphyrins and tetrabenzoporphyrins.<sup>6a</sup> Soon after that his group<sup>6</sup> and the group from Belarus<sup>7</sup> published first reports on the luminescence of tetrabenzoporphyrin complexes. In more recent years, several in-depth theoretical studies<sup>9</sup> provided insights into the electronic structure of  $\pi$ -extended tetrapyrroles, focusing mainly on their ground-state absorption spectra. For example, combined influence of  $\pi$ -extension and *meso*-tetraarylation on the spectra of tetrabenzo- and tetranaphthoporphyrins has been examined.<sup>10</sup>

In spite of these advances, effects of  $\pi$ -extension on the excited-state properties of porphyrins have been studied only scarcely, notwithstanding the fact that many potential uses of  $\pi$ -extended porphyrins rely on their singlet and triplet excited states. One particular question, much discussed in relation to regular porphyrins, is the interplay between the macrocycle structural deformations and its photophysics.<sup>11–13</sup> Although fluorescence and phosphorescence of tetrabenzoporphyrins<sup>2,1a–c,7,8,10,14</sup> and tetranaphthoporphyrins<sup>15</sup> has been mentioned in a number of publications, relationships between structural features and excited-state properties of these porphyrins have never been studied systematically. Such structure/property analysis could not be done because structural information on  $\pi$ -extended porphyrins was extremely limited,<sup>16,17</sup> in part due to their poor synthetic availability.

Over the past several years, a general method of synthesis of tetrabenzoporphyrins has been developed, based on the oxidative aromatization of porphyrins, annealed with nonaromatic hydrocarbon rings.<sup>18</sup> This method provides an access to *meso*-tetraaryl-tetrabenzo-<sup>18a,b</sup> and tetranaphthoporphyrins (Ar<sub>4</sub>TBP's and Ar<sub>4</sub>TNP's)<sup>18c,d</sup> as well as to *meso*-unsubstituted tetrabenzo- and tetranaphthoporphyrins (TBP's and TNP's).<sup>18e</sup> A recent modification of the method, based on the use of 4,7-dihydroisindole,<sup>18f</sup> also opened a pathway to 5,15-diaryl-tetrabenzoporphyrins (Ar<sub>2</sub>TBP).<sup>18g</sup> In all these cases, various functional groups can be added to the TBP macrocycles, increasing their solubility and facilitating crystal growth for X-ray structure determination. As a result, originally scarce structural information became more complete, enabling structure/property studies in the family of  $\pi$ -extended porphyrins.

In this work we analyzed photophysical properties of tetrabenzoporphyrins substituted with different numbers of *meso*-aryl groups. *meso*-Arylation is known to induce structural deformations in  $\beta$ -substituted porphyrins,<sup>19</sup> and, therefore, it can be used to study effects of macrocycle distortions on tetrabenzoporphyrin photophysics. In particular, we focused on fluorescent free-base TBP's, Ar<sub>2</sub>TBP's and Ar<sub>4</sub>TBP's and the corresponding phosphorescent Pd complexes, which to us present a special interest as near-infrared optical probes for biological imaging of oxygen.<sup>2</sup>

Effects of nonplanarity on the photophysics of regular porphyrins were systematically studied by Holten and co-workers,<sup>13</sup> who elucidated deactivation pathways of singlet excited <sup>1</sup>( $\pi$ ,  $\pi^*$ ) states (S1) of nonplanar free-bases,<sup>13a,b,d,f,h</sup> Zn porphyrins,<sup>13d</sup> Ni porphyrins<sup>13c,e</sup> and porphyrin dications.<sup>13g</sup> Formation and deactivation of triplet <sup>3</sup>( $\pi$ ,  $\pi^*$ ) states (T1) in nonplanar porphyrins has also been addressed,<sup>20</sup> including recent studies of nonplanar Pt and Pd porphyrins.<sup>21</sup> In the present paper we compared tetrabenzoporphyrins Ar<sub>n</sub>TBP ( $n = 0, 2, 4$ ) with porphyrins annealed with nonaromatic cyclohexeno-rings, i.e. tetracyclohexenoporphyrins (Ar<sub>n</sub>TCHP's, ( $n = 0, 2, 4$ )). These were chosen among other  $\beta$ -alkyl-substituted porphyrins because of their close structural similarity to Ar<sub>n</sub>TBP's. This comparison enabled us to directly evaluate  $\pi$ -extension as a factor influencing photophysics of nonplanar porphyrins.

## Results and Discussion

In the beginning we briefly summarize relevant facts about the photophysics and structures of conformationally distorted porphyrins. For detailed discussion see refs.<sup>11, 13, 19</sup>

The most common way to induce structural deformations in synthetic porphyrins<sup>19</sup> is to position several bulky substituents at the macrocycle periphery. Steric repulsion between the  $\beta$ -pyrrole groups and *meso*-substituents leads to deviations of the macrocycle from its highly symmetrical  $D_{2h}$  (free-base porphyrins) or  $D_{4h}$  (metalloporphyrin) form. Macrocycle deformations fall into two main categories: in-plane (ip) and out-of-plane distortions (oop). There are several ways to quantify these distortions; however, the most general method is to decompose the macrocycle structure in the basis of distortions corresponding to the normal vibrational modes. The Normal mode Structural Decomposition (NSD) analysis, developed by Shelnutz and co-workers,<sup>22</sup> quantifies not only the total in-plane and out-of-plane displacements ( $D_{ip}$  and  $D_{oop}$ ), but distinguishes between individual contributions of different distortion modes,<sup>22,19</sup> which are known to affect the photophysics of nonplanar porphyrins differently.<sup>13a,b</sup>

Distorted porphyrins typically exhibit mixtures of distortion modes; however, each structure is usually dominated by a single prevalent type of distortion. For example, out-of-plane distorted porphyrins are usually either mostly saddled ( $B_{2u}$ -deformation, e.g., octaethyltetraphenylporphyrin (OETPP) or dodecaphenylporphyrin (DPP)) or ruffled ( $B_{1u}$ -deformation, e.g., *meso*-tetra-*tert*-butylporphyrin (T(*t*-Bu)P)).<sup>23,19</sup>

Compared to planar porphyrins, such as octaethylporphyrin (OEP) or tetraphenylporphyrin (TPP), out-of-plane distorted porphyrins exhibit red-shifted and broadened optical spectra. The origin of red shifts in the spectra of nonplanar porphyrins has been extensively discussed in the literature.<sup>11,12f-h</sup> In *meso*-tetraarylporphyrins the red shifts at least in part are caused by an increase in the conjugation between the macrocycle and *meso*-aryl substituents.<sup>10,24</sup> In nonplanar porphyrins, the *meso*-aryl groups are rotated to a less than 90° angle with respect to the macrocycle average plane.

Nonplanar deformations of porphyrins also strongly affect properties of excited states. Both saddling and ruffling broaden the emission spectra and induce progressively large Stokes shifts with increasing degree of nonplanarity.<sup>13</sup> Saddle-shaped freebase porphyrins (e.g., H<sub>2</sub>OETPP and H<sub>2</sub>DPP) typically exhibit S<sub>1</sub> lifetimes ( $\tau_{fl}$ ) of about 0.5–1.0 ns and fluorescence quantum yields ( $\phi_{fl}$ ) in the order of 0.005 at room temperature.<sup>11,13a</sup> Ruffled free-base porphyrins have even shorter singlet lifetimes (e.g.,  $\tau_{fl} = 50$  ps for H<sub>2</sub>T(*t*-Bu)P) and negligible emission yields ( $\phi_{fl} < 0.0001$ ).<sup>13b</sup> For comparison, singlet lifetimes and fluorescence quantum yields of the planar analogues (e.g., H<sub>2</sub>OEP or H<sub>2</sub>TPP) are 10–15 ns and 0.1–0.2, respectively, while their internal conversion quantum yields are in the range  $\phi_{ic} \approx 0.1$ .<sup>13,25,26</sup> Short S<sub>1</sub> lifetimes of nonplanar porphyrins were shown to be affiliated with enhancements of both S<sub>1</sub> → S<sub>0</sub> internal conversion and S<sub>1</sub> → T<sub>1</sub> intersystem crossing.<sup>12c</sup> Polar solvents further increase the Stokes shifts, shorten the lifetimes and decrease the fluorescence quantum yields of nonplanar porphyrins,<sup>13h</sup> while lowering the temperature has the opposite effect, especially in the case of ruffled porphyrins.<sup>13d</sup>

Holten and co-workers rationalized these findings by considering increased conformational flexibility of nonplanar porphyrins in their S<sub>0</sub> and S<sub>1</sub> states.<sup>13</sup> Broadening of the absorption and fluorescence spectra and large fluorescence Stokes shifts were associated with the existence of multiple excited-state conformations, easily accessible *via* low-energy out-of-plane vibrations. Some of these conformations can form so-called *funnels*<sup>27</sup> on the S<sub>1</sub> potential energy surface, separated from the global energy minimum by small kinetic barriers. Rapid

internal conversion occurring in the funnels is due to the small  $S_1$ – $S_0$  energy gaps and favorable Franck–Condon factors, corresponding to out-of-plane vibrations. In addition, intersystem crossing near the funnels also can be enhanced. On the contrary, fluorescence occurs away from the funnels (e.g., near the global  $S_1$  minimum), where the  $S_1$ – $S_0$  gaps are quite large.

The photophysical properties of tetrabenzoporphyrins are discussed below within the framework of this model.

### Free-Base $Ar_n$ TBP's and $Ar_n$ TCHP's ( $n = 0, 2, 4$ )

The structures of porphyrins studied in this work are summarized in Chart 1 (see Supporting Information, II for details of synthesis).

The optical absorption and fluorescence spectra of free-base  $Ar_n$  TBP's ( $n = 0, 2, 4$ ) are shown in Figure 1 (upper row). The spectra of the similarly substituted *meso*-aryl tetracyclohexenoporphyrins ( $Ar_n$  TCHP's,  $n = 0, 2, 4$ ) are shown in the bottom row, and all the photophysical data are summarized in Table 1. All the measurements were performed in air-equilibrated toluene or dimethylacetamide (DMA) (noted) solutions at 295 K, except that: 1) to overcome solubility problems,  $H_2$ TBP (**1**) was first dissolved in pyridine, and a drop of this solution was added to about 5 mL of toluene; 2) a small amount of TMEDA (tetramethylethylenediamine) was added to the solution of  $H_2$ Ph<sub>4</sub>TCHP (**6**) to avoid protonation, since  $H_2$ Ar<sub>4</sub>TCHP's are known to possess very high basicities.<sup>28</sup> Due to its improved solubility,  $H_2$ TCHP (**4**), substituted with eight butoxycarbonyl groups, was used in our experiments instead of unsubstituted  $H_2$ TCHP. The effect of the butoxycarbonyl groups on the macrocycle  $\pi$ -system in  $H_2$ TCHP (**5**) is anticipated to be insignificant, since these substituents are separated from the macrocycle by several  $\sigma$ -bonds. In addition to free-bases shown in Figure 1, porphyrins with peripheral substituents (Chart 1) were used in some of the experiments (vide infra).

The optical absorption spectrum of planar  $H_2$ TBP (**1**) (Figure 1A) shows a well-resolved vibronic structure in the Q-band region and a large splitting,  $841\text{ cm}^{-1}$ , of the Soret band. This splitting is caused by the strong mixing of the B and Q states and relatively high intensity of the Q-bands.<sup>6a,9b,c</sup> The lowest energy Q-band (663 nm) is red-shifted by 39 nm ( $943\text{ cm}^{-1}$ ) relative to the corresponding transition of the also planar (vide infra)<sup>29</sup>  $H_2$ TCHP (**4**) (Figure 1D) due to the effect of extended  $\pi$ -conjugation.<sup>9,10</sup>

Both  $H_2$ TBP (**1**) and  $H_2$ TCHP (**4**) exhibit small fluorescence Stokes shifts ( $45\text{ cm}^{-1}$  and  $25.6\text{ cm}^{-1}$ ), indicating rigid planar structures. In good agreement with the previously published data,<sup>1b,8c</sup>  $H_2$ TBP (**1**) shows a very high for porphyrins fluorescence quantum yield ( $\phi_{fl} = 0.35$  in toluene), while the yield of  $H_2$ TCHP (**4**) is significantly lower ( $\phi_{fl} = 0.14$ ), nearly matching that of  $H_2$ OEP ( $\phi_{fl} = 0.16$ ). The  $S_1$  lifetime of  $H_2$ TBP (**1**) (9.8 ns) is shorter than that of  $H_2$ TCHP (**4**) (14.1 ns). The calculated values of the corresponding rate constants are presented in Table 2. An almost 3.6 times higher value of the radiate rate constant ( $k_r$ ) for  $H_2$ TBP (**1**) agrees well with much higher oscillator strength of its Q-band transition ( $\log \epsilon(663\text{ nm}) = 4.22$  for  $H_2$ TBP (**1**) vs  $\log \epsilon(624\text{ nm}) = 3.70$  for  $H_2$ TCHP (**4**)).<sup>18e</sup>

The quantum yield of the nonradiative decay ( $\phi_{nr} = \phi_{ic} + \phi_{isc}$ ;  $\phi_{ic}$ , internal conversion;  $\phi_{isc}$ , intersystem crossing) for  $H_2$ TCHP (**4**) ( $\phi_{nr} = 0.86$ ) is higher than that for  $H_2$ TBP (**1**) ( $\phi_{nr} = 0.65$ ), but the corresponding nonradiative rate constant ( $k_{nr} = k_{ic} + k_{isc}$ ) for  $H_2$ TCHP (**4**) is slightly lower (Table 2). The faster nonradiative decay of  $H_2$ TBP (**1**) might be due to the higher rate of the internal conversion alone, since the  $S_1$ – $S_0$  gap for  $H_2$ TBP (**1**) is almost 1000

**Supporting Information Available:** Description of synthesis, details of photophysical experiments, computations and X-ray structure determination, as well as characterization data for the new compounds. This material is available free of charge via the Internet at <http://pubs.acs.org>.

$\text{cm}^{-1}$  narrower than that in  $\text{H}_2\text{TCHP}$  (**4**); however, it may also reflect the altered rate of intersystem crossing.

The optical properties of  $\text{H}_2\text{Ph}_4\text{TBP}$  (**3**) (Figure 1C) (strongly saddled structure, vide infra) in general follow the pattern predicted by the Holten's model.<sup>13</sup> Upon going from  $\text{H}_2\text{TBP}$  (**1**) to  $\text{H}_2\text{Ph}_4\text{TBP}$  (**3**), the fine vibronic structure of the Q-band disappears, and both bands shift to the red: Q-band by  $736\text{ cm}^{-1}$ , Soret band by  $2163\text{ cm}^{-1}$ . Similar trends are seen in the absorption spectrum of also saddled (vide infra)  $\text{H}_2\text{Ph}_4\text{TCHP}$  (**6**) (Figure 1F) vs planar  $\text{H}_2\text{TCHP}$  (**4**) (Figure 1D). The two latter spectra closely resemble the published spectra of  $\text{H}_2\text{OETPP}$  and  $\text{H}_2\text{OEP}$ , respectively.<sup>13a,26</sup>

The changes in the fluorescence of  $\text{H}_2\text{Ph}_4\text{TBP}$  (**3**) vs that of  $\text{H}_2\text{TBP}$  (**1**) in general also conform to the model (see Table 1). For example, the fluorescence quantum yield of  $\text{H}_2\text{Ph}_4\text{TBP}$  (**3**) is lower than that of  $\text{H}_2\text{TBP}$  (**1**) by about 10 times, almost matching the change in the pair  $\text{H}_2\text{Ph}_4\text{TCHP}$  (**6**)/ $\text{H}_2\text{TCHP}$  (**4**). The Stokes shift of  $\text{H}_2\text{Ph}_4\text{TBP}$  (**3**) ( $162.8\text{ cm}^{-1}$ ) is somewhat lower than that of  $\text{H}_2\text{Ph}_4\text{TCHP}$  (**6**) ( $670\text{ cm}^{-1}$ ), and upon changing the solvent to more polar DMA it increases by 36% (to  $223\text{ cm}^{-1}$ ). The Stokes shift for  $\text{H}_2\text{Ph}_4\text{TCHP}$  (**6**) increases in DMA by almost the same value (to  $882\text{ cm}^{-1}$ ).

Typical of nonplanar porphyrins,<sup>13h</sup> the fluorescence quantum yield of  $\text{H}_2\text{Ph}_4\text{TBP}$  (**3**) decreases in more polar solvent and its emission spectrum broadens (see Supporting Information, III). Interestingly, the fluorescence quantum yields of planar  $\text{H}_2\text{TBP}$  (**1**) increases in DMA to 0.47—a change not normally observed for planar porphyrins.

The dynamic fluorescence data for the most part are consistent with the steady-state measurements. The fluorescence decays of both  $\text{H}_2\text{Ph}_4\text{TBP}$  (**3**) and  $\text{H}_2\text{Ph}_4\text{TCHP}$  (**6**) reveal broad underlying distributions of lifetimes (recovered by the Maximum Entropy Method (MEM),<sup>30</sup> Figure 2), which are indicative of multiple excited-state conformations in agreement with the model. The radiative rate constants ( $k_r$ ) (Table 2) decrease by about 3.3 times on going from  $\text{H}_2\text{TBP}$  (**1**) to  $\text{H}_2\text{Ph}_4\text{TBP}$  (**3**) and by about 2.6 times on going from  $\text{H}_2\text{TCHP}$  (**4**) to for  $\text{H}_2\text{Ph}_4\text{TCHP}$  (**6**). Therefore, low  $S_1$  lifetimes (see Table 1) of both *meso*-tetraarylated porphyrins are due to the strong enhancement of the nonradiative processes. Indeed, the corresponding rate constants ( $k_{nr}$ ) increase by 6.2 times from  $\text{H}_2\text{TCHP}$  (**4**) to  $\text{H}_2\text{Ph}_4\text{TCHP}$  (**6**) and by only slightly less, i.e. 5.2 times, from  $\text{H}_2\text{TBP}$  (**1**) to  $\text{H}_2\text{Ph}_4\text{TBP}$  (**3**). Notably, the nonradiative rate for  $\text{H}_2\text{OETPP}$  is significantly higher, i.e.,  $k_{nr}$ )  $1.5 \times 10^9\text{ s}^{-1}$ ,<sup>13a</sup> than for  $\text{H}_2\text{Ph}_4\text{TCHP}$ .

The main conclusion drawn from these comparisons is that  $S_1$  states of nonplanar porphyrins are significantly less prone to nonradiative deactivation when these porphyrins are annealed with cyclic motifs (as in  $\text{H}_2\text{Ph}_4\text{TCHP}$  (**6**)) as opposed to  $\beta$ -substituted with pendant alkyl groups (as in  $\text{H}_2\text{OETPP}$ ). In addition, if the cyclic motifs are in conjugation with the macrocycle (as in  $\text{H}_2\text{Ph}_4\text{TBP}$  (**3**)), the nonradiative decay appears to weaken even more, although within the measurement error. The differences between nonradiative rates of these three types porphyrins can be explained by taking into account that their  $S_0$ - $S_1$  gaps change in parallel with their rate constants  $k_{nr}$ , i.e.,  $\text{H}_2\text{Ph}_4\text{TBP} \approx \text{H}_2\text{Ph}_4\text{TCHP} < \text{H}_2\text{OETPP}$ . However, the observed effect may also be related to higher rigidity of macrocycles annealed with exocyclic fragments, especially with benzo- rings.

It has been shown that photophysical properties of free-base porphyrins change gradually with increasing degree of the macrocycle nonplanarity.<sup>12a,13h</sup> Therefore, one could expect that tetrabenzoporphyrins substituted with two, as opposed to four, *meso*-aryl groups would exhibit optical properties somewhat average to those of  $\text{H}_2\text{TBP}$ 's and  $\text{H}_2\text{Ar}_4\text{TBP}$ 's. In contrast to this expectation, the absorption spectrum of  $\text{H}_2\text{Ph}_2\text{TBP}$  (**2**) (Figure 1B) appears to be nearly

identical to that of H<sub>2</sub>TBP (**1**), with the Q and Soret bands only slightly shifted to the red, by 5 and 10 nm, respectively.<sup>31</sup>

The vibronic structure of the Q-band of H<sub>2</sub>Ph<sub>2</sub>TBP (**2**) and the shape of its Soret band are identical to those of H<sub>2</sub>TBP (**1**), except for a small extra peak at 449 nm in the spectrum of the latter. This peak is likely to be caused by an impurity. A similar feature was observed in the spectrum of H<sub>2</sub>TBP<sup>8d</sup> synthesized by the template condensation method.<sup>32</sup> The method is known to yield complex mixtures of products. On the other hand, the spectrum of well-soluble octabutoxy-derivative H<sub>2</sub>TBP(CO<sub>2</sub>Bu)<sub>8</sub> did not show this extra feature (see Supporting Information, III).

The fluorescence properties of H<sub>2</sub>TBP (**1**) and H<sub>2</sub>Ph<sub>2</sub>TBP (**2**) are also very close: small Stokes shifts (~45 cm<sup>-1</sup>), long fluorescence lifetimes (9.8 and 10.3 ns) and high emission yields (0.35 and 0.34), increasing to 0.47 and 0.41, respectively, in DMA.

Similarities in the optical properties of H<sub>2</sub>Ph<sub>2</sub>TBP (**2**) and H<sub>2</sub>TBP (**1**) suggest that the structures of these porphyrins should also be similar, i.e. that H<sub>2</sub>Ph<sub>2</sub>TBP (**2**) should be planar. On the other hand, based on the published data,<sup>16,18a,b,28</sup> H<sub>2</sub>Ph<sub>4</sub>TBP (**3**) is expected to be strongly nonplanar, presumably saddled. The question arises as to why the interactions between *meso*-aryl rings and benzo-rings in H<sub>2</sub>Ph<sub>2</sub>TBP (**2**) do not affect its planarity, whereas the same interactions in H<sub>2</sub>Ph<sub>4</sub>TBP cause it to become strongly nonplanar?

In order to perform structural comparisons we carried out DFT (B3LYP/6-31G(d)) calculations of porphyrins depicted in Figure 1. The calculated structures are shown in Figure 3 together with their normal distortion modes, as revealed by the NSD analysis.<sup>22</sup> It should be mentioned that the X-ray structures of H<sub>2</sub>TBP (**1**) cations (planar),<sup>17</sup> unsubstituted H<sub>2</sub>TCHP (anomalously planar dication)<sup>29</sup> and H<sub>2</sub>Ph<sub>4</sub>TBP(CO<sub>2</sub>Me)<sub>8</sub> (saddled)<sup>28</sup> were published in the literature, providing the required reference points. However, for the purpose of the comparative analysis, computed structures may in fact present an advantage, since X-ray structures are potentially affected by crystal packing forces, which may or may not affect the macrocycle's planarity.

It is seen from the figure that the macrocycle of H<sub>2</sub>Ph<sub>2</sub>TBP (**2**) is as planar as that of H<sub>2</sub>TBP (**1**). The total out-of-plane displacements ( $D_{oop}$ ) are practically zero for both porphyrins. The phenyl rings in H<sub>2</sub>Ph<sub>2</sub>TBP (**1**) are strictly orthogonal to the macrocycle plane and, as a result, their effect on the macrocycle electronic system is minor. Indeed, the absorption bands of H<sub>2</sub>Ph<sub>2</sub>TBP (**2**) are only slightly red-shifted vs those of H<sub>2</sub>TBP (**1**), and the substituents in the *meso*-phenyl rings, e.g., *para*-methoxycarbonyl groups in porphyrin **2a** (Chart 1), have negligible effect on the peak positions (see Supporting Information, III).

As expected, the structure of H<sub>2</sub>Ph<sub>4</sub>TBP (**3**) is strongly nonplanar ( $D_{oop} = 3.02 \text{ \AA}$ ), with B<sub>2u</sub>-saddling mode being the dominant deformation. H<sub>2</sub>Ph<sub>4</sub>TCHP (**6**) is also saddled, but with a contribution of ruffling (B<sub>1u</sub>). B<sub>1u</sub>-mode is known to especially strongly enhance nonradiative decay of the S<sub>1</sub> state,<sup>13b</sup> suggesting that the steeper increase in  $k_{nr}$  (vide supra) upon going from H<sub>2</sub>TCHP (**4**) to H<sub>2</sub>Ph<sub>4</sub>TCHP (**6**) vs the pair H<sub>2</sub>TBP (**2**)/H<sub>2</sub>Ph<sub>4</sub>TBP (**3**), may be associated with this particular distortion. The *meso*-phenyl rings in H<sub>2</sub>Ph<sub>4</sub>TBP (**3**) are tilted with respect to the macrocycle, and, therefore, are partially drawn into conjugation. As a result, *para*-methoxycarbonyl groups in **3a** shift its spectrum by 4–5 nm to the red relative to H<sub>2</sub>Ph<sub>4</sub>TBP (**3**) (see Supporting Information, III).

The intrinsic asymmetry of free-base porphyrins manifests itself in all the calculated structures by the A<sub>1g</sub>-distortion, i.e., the elongation in the direction of the axis connecting the two opposite NH nitrogen atoms. In addition to that, H<sub>2</sub>Ph<sub>2</sub>TBP (**2**) and H<sub>2</sub>Ph<sub>2</sub>TCHP (**5**) exhibit strong B<sub>2g</sub> mode, which is associated with the in-plane rotation of the isoindole fragments, leading

to the change in the distances between the opposite pairs of pyrrole N-atoms and yielding more space for the *meso*-aryl substituents. This rotation appears to lift the steric hindrance between the *meso*-aryl groups and the  $\alpha$ -hydrogen atoms ( $H_\alpha$ ) of the benzo ( $H_2Ph_2TBP$  (**2**)) or cyclohexeno rings ( $H_2Ph_2TCHP$  (**5**)). For example, the edges of the rectangular, drawn through the corresponding  $\alpha$ -carbon atoms of benzo-rings in  $H_2Ph_2TBP$  (**2**), are 5.41 and 6.12 Å ( $D_{ip} = 0.82\text{Å}$ ), while in symmetrical  $H_2TBP$  (**1**) the corresponding distances are equal (5.76 Å).

Relief of the steric strain by way of in-plane as opposed to out-of-plane deformation appears to be more energetically favorable, suggesting that it might be a more effective way to preserve the macrocycle aromaticity. Interestingly, the structure of  $H_2Ph_2TCHP$  (**5**) in addition to being distorted in-plane ( $D_{oop} = 0.75\text{Å}$ ) also shows a small contribution of saddling ( $B_{2u}$ ) ( $D_{oop} = 0.36\text{Å}$ ). This distortion is completely absent in the structure of  $H_2Ph_2TBP$  (**3**), even though the distance between the  $H_R$ -atom of the benzo-ring and the plane of the *meso*-phenyl ring (Figure 3) is actually shorter than the average distance between the *meso*-phenyl ring and the  $H_\alpha$ -atoms of the cyclohexeno-ring in  $H_2Ph_2TCHP$  (**5**). Higher resistance of  $H_2Ph_2TBP$  (**2**) to nonplanar distortion may be another manifestation of the increased rigidity of TBP macrocycle. In this regard, in a recent theoretical study<sup>24</sup> the propensity of *meso*-aryl-substituted porphyrins to undergo nonplanar deformations was considered to be an effect of two counterbalancing forces: one acting to preserve planarity and aromaticity and another striving to bring the *meso*-aryl group into conjugation with the tetrapyrrole system. From this point of view, the former force in  $H_2Ph_2TBP$  (**2**) appears to be stronger than in  $H_2Ph_2TCHP$  (**5**).

Remarkably, even a small out-of-plane deformation of  $H_2Ph_2TCHP$  (**5**) immediately reveals itself in its photophysical behavior. The absorption bands of  $H_2Ph_2TCHP$  (**5**) (Figure 2E) are broadened and red-shifted relative to  $H_2TCHP$  (**4**), the fluorescence spectrum of  $H_2Ph_2TCHP$  (**5**) has a somewhat different shape, and its fluorescence yield (0.08) and lifetime (11.8 ns) are considerably lower than those of  $H_2TCHP$  (**4**). The nonradiative rate constant for  $H_2Ph_2TCHP$  (**5**) (Table 2) increases by about 30% relative to  $k_{nr}$  of  $H_2TCHP$  (**4**), and the radiative constant decreases by about 50% relative to  $k_r$  of  $H_2TCHP$  (**4**). In contrast to these changes, the in-plane distortion in  $H_2Ph_2TBP$  (**2**) has practically no influence on the  $S_1$  decay parameters optical properties as compared to  $H_2TBP$  (**1**). These results strongly suggest that out-of-plane deformations play the dominant role in the excited-state properties of distorted porphyrins, whereas the role of in-plane deformations is insignificant.

To the best of our knowledge, the X-ray structure of  $H_2Ph_2TCHP$  (**2**) is not known. To verify that the computations adequately represented its structural features, we compared the calculated (B3LYP/6-31G(d)) structure of another 5,15-diphenyl-octalkylporphyrin with its published X-ray structure<sup>33</sup> (see Supporting Information, V). The results confirmed that all the main features of the experimental structure were adequately reproduced by the calculations. It also should be mentioned, that most of the published X-ray structures of free-base  $\beta$ -alkyl-5,15-diarylporphyrins (obtained from Cambridge Structural Database) (see ref<sup>33</sup> and Supporting Information, IV) reveal certain degree of out-of-plane deformations, although in some cases these could be caused by structural elements (e.g., strapping substituents) capable of inducing out-of-plane distortions independent of *meso*-aryl/ $\beta$ -alkyl interactions.

The experimental evidence of virtually ideal planarity of  $H_2Ar_2TBP$  as well as of its strong in-plane distortion was obtained by X-ray crystallography (Figure 4).

The crystal structure of  $H_2Ar_2TBP$  (Ar = 3,5-tBu<sub>2</sub>-C<sub>6</sub>H<sub>3</sub>) shows the essentially flat tetrapyrrole skeleton, practically orthogonal *meso*-aryl rings and significant  $A_{1g}$  and  $B_{2g}$  deformations ( $D_{ip} = 0.67\text{Å}$ ). The  $N_4$ -core is asymmetrical with adjacent edges of 3.18 and 2.76 Å. Overall, the structure is in excellent agreement with the calculations.

It follows from the above results that the spectroscopic signature of *meso*-unsubstituted TBP is as a sensitive indicator of planarity of TBP-based systems. For example, it is likely that the structures of H<sub>2</sub>ArTBP and 5,10-H<sub>2</sub>Ar<sub>2</sub>TBP, reported by Senge and Bischoff,<sup>34</sup> as well as the structure of H<sub>2</sub>ArTBP (Ar = 4-MeO<sub>2</sub>C-C<sub>6</sub>H<sub>4</sub>), reported by Berova et al.,<sup>35</sup> are planar. Similarly, *meso*-alkenyl-TBP's, synthesized by Ono et al.,<sup>36</sup> also are expected to be planar.

In summary of this section, planar free-base tetrabenzoporphyrins are strongly fluorescent and their radiative rate constants and quantum yields are 3–4 times higher than those of regular planar porphyrins. Nonplanar distortions affect the excited-state properties of free-base tetrabenzoporphyrins in a manner consistent with the model proposed for regular nonplanar porphyrins.<sup>13</sup> In contrast to out-of-plane deformations, in-plane deformations, induced in tetrabenzoporphyrins by 5,15-diaryl-substitution, have practically no effect on their excited-state properties of tetrabenzoporphyrins.

### PdAr<sub>n</sub>TBP's and PdAr<sub>n</sub>TCHP (*n* = 0, 2, 4)

In Pd porphyrins, S<sub>1</sub>(π, π\*) → T<sub>1</sub>(π, π\*) intersystem crossing occurs with almost unity quantum yield.<sup>37</sup> Because (*d, d*) transitions of Pd(II) ion are higher in energy than T<sub>1</sub>(π, π\*) states, planar Pd porphyrins (e.g., PdOEP, PdTPP) strongly phosphoresce in solutions at room temperature.<sup>38</sup>

Recently, Zenkevich and co-workers<sup>21</sup> showed that saddling (B<sub>2u</sub>) deformations in regular Pd porphyrins, such as PdOETPP,<sup>39,40</sup> lead to a drastic decrease in their phosphorescence, whereas at low temperatures the phosphorescence is considerably regained (φ<sub>phos</sub>=0.25 for PdOETPP at 77 K).<sup>21b</sup> Having that in mind, we set out to examine how *meso*-aryl substituents in PdAr<sub>n</sub>TBP's (*n* = 0, 2, 4) affect properties of their T<sub>1</sub> states. As in the case of free-base porphyrins, Pd complexes of structurally related Ar<sub>n</sub>TCHP's (*n* = 0, 2, 4) (Chart 1) were used for comparison.

Structural information on Pd porphyrins is not as easily obtainable by ab initio methods as for free-bases. Nevertheless, previously published structural data on various types of metallated planar and nonplanar porphyrins allowed us to make the following conjectures. Similar to PdOEP,<sup>41</sup> PdTCHP (**Pd-4**) is expected to have unperturbed planar geometry. Literature data on Cu, Co and Zn tetrabenzoporphyrins<sup>4b-d</sup> suggest that PdTBP (**Pd-1**) also has planar geometry. Similar to Cu, Zn and Ni OETPP's,<sup>40</sup> PdPh<sub>4</sub>TCHP (**Pd-6**) is expected to be saddled; while based on the existing X-ray data on metallated 5,15-diaryl β-octaalkylporphyrins,<sup>42</sup> PdPh<sub>2</sub>TCHP is expected to be predominantly ruffled.

By analogy with regular 5,15-diarylporphyrins, we expected that metalation of Ar<sub>2</sub>TBP's would change the geometry of the N<sub>4</sub>-core and, as a result, would lead to a closer contact between benzo and *meso*-aryl rings. Metallated β-alkyl 5,15-diarylporphyrins typically undergo nonplanar B<sub>1u</sub>-type ruffling deformation,<sup>42</sup> and the same was expected for PdPh<sub>2</sub>TBP (**Pd-2**). The X-ray structure of PdPh<sub>2</sub>TBP (**Pd-2**) (Figure 5 A) confirmed this expectation. The predominant mode of its out-of-plane distortion (*D*<sub>oop</sub> = 1.08 Å) is indeed ruffling (B<sub>1u</sub>) with a small contribution of saddling (B<sub>2u</sub>), while the in-plane distortion is much smaller (*D*<sub>ip</sub> = 0.19 Å) than in the corresponding free-base H<sub>2</sub>Ph<sub>2</sub>TBP (**2**) (Figure 1 and Figure 4).

PdAr<sub>4</sub>TBP (Ar = 3,5-(BuO<sub>2</sub>C)<sub>2</sub>C<sub>6</sub>H<sub>3</sub>) (Figure 5B) is, on the contrary, strongly saddled. The value of the total out-of-plane deformation in PdAr<sub>4</sub>TBP (*D*<sub>oop</sub> = 2.32 Å) is similar to that determined for the earlier published structure of ZnPh<sub>4</sub>TBP·THF (*D*<sub>oop</sub> = 2.35 Å),<sup>16</sup> but somewhat lower than in PtPh<sub>4</sub>TBP (*D*<sub>oop</sub> = 2.83 Å)<sup>4e</sup> and especially in NiPh<sub>4</sub>TBP (CO<sub>2</sub>Me)<sub>8</sub> (*D*<sub>oop</sub> = 3.43 Å).<sup>18b</sup> These differences might be caused by the differences in ionic radii of the metals or by the crystal packing forces or by both.



The optical spectra of PdPh<sub>n</sub>TBP's and PdPh<sub>n</sub>TCHP's ( $n = 0, 2, 4$ ) are shown in Figure 6, and the photophysical data are summarized in Table 3. The phosphorescence quantum yields and decays were measured in Ar-purged DMA solutions at 295 K, and the phosphorescence decays were found to be purely single-exponential. Porphyrin triplet states are extremely sensitive to various quenching processes, and that makes it difficult to compare the data on the phosphorescence of Pd porphyrins measured in different laboratories using different solvents and different deoxygenation methods. Therefore, in our experiments we attempted to maintain identical conditions (solvent, Ar purity, control of air displacement) for all the samples measured; however, the reported lifetimes and quantum yields should not be considered absolute.

Unsubstituted PdTBP (**Pd-1**) has very low solubility and shows tendency to aggregation. To account for possible effects of aggregation, a well-soluble PdTBP derivative substituted with eight butoxycarbonyl groups, PdTBP(CO<sub>2</sub>Bu)<sub>8</sub> (**Pd-1a**), was also studied. It should be mentioned that insertion of Pd into Ar<sub>n</sub>TCHP's often leads to the appearance of extra bands above 600 nm in the absorption spectra. These bands are most likely associated with partially oxidized products, i.e. mono-, di- and tribenzoporphyrins. Special care needs to be taken to avoid contamination by these side products, and only freshly prepared and purified samples of PdPh<sub>2</sub>TCHP (**Pd-5**) must be used in photophysical measurements.

The changes in the ground-state absorption spectra of PdAr<sub>n</sub>TBP's and PdAr<sub>n</sub>TCHP's upon increase in  $n$  from 0 to 4 resemble the trends observed for the corresponding free-bases: red-shifting, broadening and, in the case of PdAr<sub>n</sub>TCHP's, gradual change in the relative intensity of Q<sub>x</sub> vs Q<sub>y</sub> band. As expected, the spectrum of PdAr<sub>4</sub>TCHP (**Pd-6**) was found to be similar to the published spectrum of PdOETPP.<sup>21</sup> Noteworthy, there is a slight splitting of the Q-band ( $\lambda_{\max} = 615$  nm) of PdAr<sub>2</sub>TBP (**Pd-2**), a feature absent in the spectrum of PdTBP (**Pd-1**).

The phosphorescence spectra in general follow the changes in the absorption. One exception is that the main peak of the phosphorescence of ruffled PdPh<sub>2</sub>TBP (**Pd-2**) ( $\lambda_{\max} = 796$  nm) is located almost at the same position as that of saddled PdPh<sub>4</sub>TBP (**Pd-3**) ( $\lambda_{\max} = 797$  nm), while the Q-bands shift gradually in the order PdTBP (**Pd-1**) → PdPh<sub>2</sub>TBP (**Pd-2**) → PdPh<sub>4</sub>TBP (**Pd-3**). As a result, the phosphorescence Stokes shift of PdPh<sub>4</sub>TBP (**Pd-3**) is less by more than 200 cm<sup>-1</sup> compared to the two less substituted porphyrins.

The major difference between PdAr<sub>n</sub>TBP's and PdAr<sub>n</sub>TCHP's is in how their phosphorescence quantum yields and lifetimes respond to the changes in the macrocycle nonplanarity. Just like in the case of PdOETPP,<sup>21</sup> saddling deformation in PdAr<sub>4</sub>TCHP (**Pd-6**) leads to the complete loss of its emissivity. In contrast, saddled PdAr<sub>4</sub>TBP (**Pd-3**) phosphoresces with quite high quantum yield ( $\phi_{\text{phos}} = 0.08$ ), which is only 1.6 lower than that of planar PdTBP (**Pd-1**) ( $\phi_{\text{phos}} = 0.13$ ). It is possible that the phosphorescence yield and lifetime of PdTBP (**Pd-1**) are affected (lowered) by aggregation. Indeed, the phosphorescence of much better soluble octabutoxycarbonyl-derivative **Pd-1a** was found to be significantly stronger ( $\phi_{\text{phos}} = 0.35$ ); but still, the difference between the quantum yields of **Pd-1a** and PdAr<sub>4</sub>TBP (**Pd-3**) is not nearly as drastic as for PdPh<sub>4</sub>TCHP (**Pd-6**) vs PdTCHP (**Pd-4**).

Both radiative and nonradiative rate constants for PdTBP (**Pd-1a**) are somewhat higher than those of PdTCHP (**Pd-4**) (Table 4). In response to nonplanar deformation, the radiative rate in PdPh<sub>4</sub>TBP (**Pd-3**) decreases slightly relative to that of PdTBP (**Pd-1a**), resembling the trend in the behavior of the corresponding free-bases. Remarkably, upon going from PdTBP (**Pd-1a**) to PdPh<sub>4</sub>TBP (**Pd-3**) the nonradiative rate rises also by only about 2.7 times, whereas in PdPh<sub>4</sub>TCHP (**Pd-6**)  $k_{\text{nr}}$  is apparently so large, that this porphyrin completely loses its phosphorescence.

For PdPh<sub>2</sub>TBP (**Pd-2**) and PhPh<sub>2</sub>TCHP (**Pd-5**) the differences are also quite striking. Upon going from planar PdTCHP (**Pd-4**) to presumably ruffled PdPh<sub>2</sub>TCHP (**Pd-5**), the phosphorescence quantum yield decreases by as much as 22.5 times, while in the case of PdTBP (**Pd-1**) vs PdPh<sub>2</sub>TBP (**Pd-2**) it seems to even slightly increase. Again, this can be related to the partial aggregation of PdTBP (**Pd-1**); but even in comparison with octabutoxycarbonyl-derivative **Pd-1a**, the quantum yield of PdPh<sub>2</sub>TBP (**Pd-2**) is only 4 times lower. Notably, this decrease in the quantum yield is largely due to the decrease in the radiative rate constant, while the increase in the nonradiative rate is only 1.5 times.

Overall, the photophysical data clearly show that  $\pi$ -extension strongly affects triplet state properties of Pd porphyrins. Nonplanarity, especially saddling, greatly promotes nonradiative decay of the T<sub>1</sub> states of regular nonplanar Pd porphyrins, rendering them completely nonemissive. On the contrary, either saddling (B<sub>2u</sub>) or ruffling (B<sub>1u</sub>) deformations affect the T<sub>1</sub> states of tetrabenzoporphyrins only slightly; both PdAr<sub>2</sub>TBP's and PdAr<sub>4</sub>TBP's remain strongly phosphorescent at ambient temperatures.

Disappearance of the phosphorescence in regular nonplanar porphyrins in principle can be caused by strong enhancement of S<sub>1</sub> → S<sub>0</sub> internal conversion, leading to the reduction in the yield of the T<sub>1</sub> state. However, literature data suggest that the enhancement of internal conversion in nonplanar porphyrins occurs in parallel with the enhancement of the intersystem crossing.<sup>12c</sup> In the presence of Pd, S<sub>1</sub> → T<sub>1</sub> decay should become even faster, and, as a result, it is likely to reach the rate at least as high as that of the internal conversion. Therefore, the key factor influencing phosphorescence of nonplanar Pd porphyrins is most likely the rate of T<sub>1</sub> → S<sub>0</sub> decay.

The rates of radiative T<sub>1</sub> → S<sub>0</sub> transitions are somewhat higher for planar PdTBP's than for planar PdTCHP's, and upon nonplanar deformations they slightly decrease (vide supra). The nonradiative T<sub>1</sub> → S<sub>0</sub> rates increase sharply in response to non-planar deformations in PdTCHP's, but only slightly in PdTBP's. The fact that the phosphorescence of nonplanar Pd porphyrins, e.g. of PdOETPP, is regained at 77 K<sup>21</sup> suggests that the enhancement of the nonradiative decay is associated with vibrational activity. Thus, vibrations greatly enhance T<sub>1</sub> → S<sub>0</sub> intersystem crossing in PdAr<sub>4</sub>TCHP's, but have only small effect on the intersystem crossing in PdAr<sub>4</sub>TBP's.

The rate of T<sub>1</sub> → S<sub>0</sub> intersystem crossing is determined by the combination of three factors: spin-orbit coupling due to the heavy atom effect; interactions of Pd *d* orbitals with T<sub>1</sub> and S<sub>0</sub> states, resulting in their partial mixing; and Franck-Condon factors associated with the participating vibrational levels of the states involved.<sup>21,43</sup> It is likely that some of the low-energy out-of-plane vibrations near the equilibrium point on the T<sub>1</sub> potential energy surface facilitate spin-orbit coupling and enhance the nonradiative decay.<sup>43</sup> Even if favorable for intersystem crossing conditions are not met near the equilibrium, there are likely to be conformers (local minima) on the T<sub>1</sub> surface characterized by higher magnitudes of spin-orbit coupling. High conformational flexibility of nonplanar Pd porphyrins is likely to be retained in their T<sub>1</sub> states,<sup>20</sup> and the conformers with increased magnitude of spin-orbit coupling can be viewed as analogs of "funnels" proposed for nonradiative deactivation of S<sub>1</sub> states.<sup>13</sup> Considering low T<sub>1</sub> → S<sub>0</sub> radiative rates, the molecule has enough time to visit all these local minima, including the funnels, and undergo efficient nonradiative T<sub>1</sub> → S<sub>0</sub> decay.

The described above experiments suggest that the conformations characterized by high rates of intersystem crossing are not as easily attainable by PdAr<sub>4</sub>TBP's as by PdAr<sub>4</sub>TCHP's. On the one hand, this can be a result of lower flexibility of the PdAr<sub>4</sub>TBP system and, therefore, its limited ability to traverse the T<sub>1</sub> energy surface. However, the data on free-base Ar<sub>4</sub>TBP's

(vide supra) suggest that even if there is an increase in the rigidity of the TBP macrocycle compared to that of TCHP, the difference is not large.

Alternatively, it is possible that for all possible conformers of PdAr<sub>4</sub>TBP's the magnitude of spin-orbit coupling is never as high as for some selected conformers of PdAr<sub>4</sub>TCHP's. Should this indeed be true, the reason for much weaker effects of nonplanar deformations on the phosphorescence of PdAr<sub>4</sub>TBP's vs PdAr<sub>4</sub>TCHP's could be explained by the difference between the spatial distributions of *b*<sub>1</sub> (HOMO) and *e* (LUMO) orbitals of tetrabenzoporphyrins vs regular porphyrins.<sup>10</sup> Indeed, *b*<sub>1</sub> HOMO and *e*<sub>g</sub> LUMO orbitals in Zn and Pd Ph<sub>4</sub>TBP's were shown to be partially moved out from the pyrroles into benzo-rings,<sup>10</sup> away from the metal center. As a result, interactions of these orbitals with *d*-orbitals of Pd even in out-of-plane distorted macrocycle may be much weaker than in PdAr<sub>4</sub>TCHP's.

An interesting observation was made that the triplet lifetimes of Pd porphyrins (both TBP's and TCHP's) are affected by ruffling much less than by saddling. Noteworthy, the structures of highly phosphorescent PdTPP<sup>44</sup> and Pd *meso*-tetracarboxyphenylporphyrin<sup>45</sup> apparently are also quite ruffled. In the case of S<sub>1</sub> states of free-base porphyrins, however, the situation is exactly the opposite, i.e. nonradiative decay in ruffled porphyrins is much faster than in saddled porphyrins (vide supra). In fact, the very fast internal conversion of ruffled free-base porphyrins<sup>13b</sup> is perhaps one of strongest indications of the existence of funnels on their potential energy surfaces. Either analogous minima do not exist on T<sub>1</sub> surfaces of ruffled Pd porphyrins, or spin-orbit coupling in these minima is inefficient. A separate study will be required to understand this phenomenon.

## Conclusion

The presented data provide initial experimental framework for understanding mechanisms of photophysical processes occurring in planar and nonplanar  $\pi$ -extended porphyrins. The performed phenomenological analysis can be useful for building empirical correlations between structures and photophysical properties of these molecules and forming the initial picture; however, comprehensive computational work, such as recently performed on free-base porphyrin and its Mg and Zn complexes,<sup>43</sup> will be required to fully delineate the effects of the  $\pi$ -extension on the excited properties of nonplanar tetrapyrroles.

From practical point of view, the described photophysical measurements allowed identification of a subset of  $\pi$ -extended porphyrins, namely 5,15-diaryltetrabenzoporphyrins, which combine powerful near-infrared absorption and strong emission from singlet and triplet states with ease of derivatization via substitution in the *meso*-aryl rings. Convenient functionalization not leading to alterations in photophysical properties is the key to many potential applications of these chromophores, such as biomedical imaging and PDT.

## Experimental Section

All porphyrins used in this study were synthesized and purified as described previously,<sup>18</sup> except for complexes **Pd-4**, **Pd-5**, **Pd-5a** and **Pd-6**. The latter were obtained by refluxing the corresponding free-base porphyrins with Pd(OAc)<sub>2</sub> in acetic acid and purified by column chromatography (see Supporting Information, II for details).

Absorption and emission spectra, fluorescence and phosphorescence quantum yields and lifetimes were measured using standard methods (see Supporting Information, I). Complete X-ray crystal structures are available in the Cambridge Crystallographic Data Centre (CCDC): 665410, 681173, 687685. For details of DFT calculations see Supporting Information, V. NSD analysis<sup>22</sup> was performed using an online Java applet available at the Web site of Prof. John

A. Shelnett: <http://jasheln.unm.edu/jasheln/content/nsd/NSDEngine/start.htm> (see Supporting Information, V for details).

## Acknowledgment

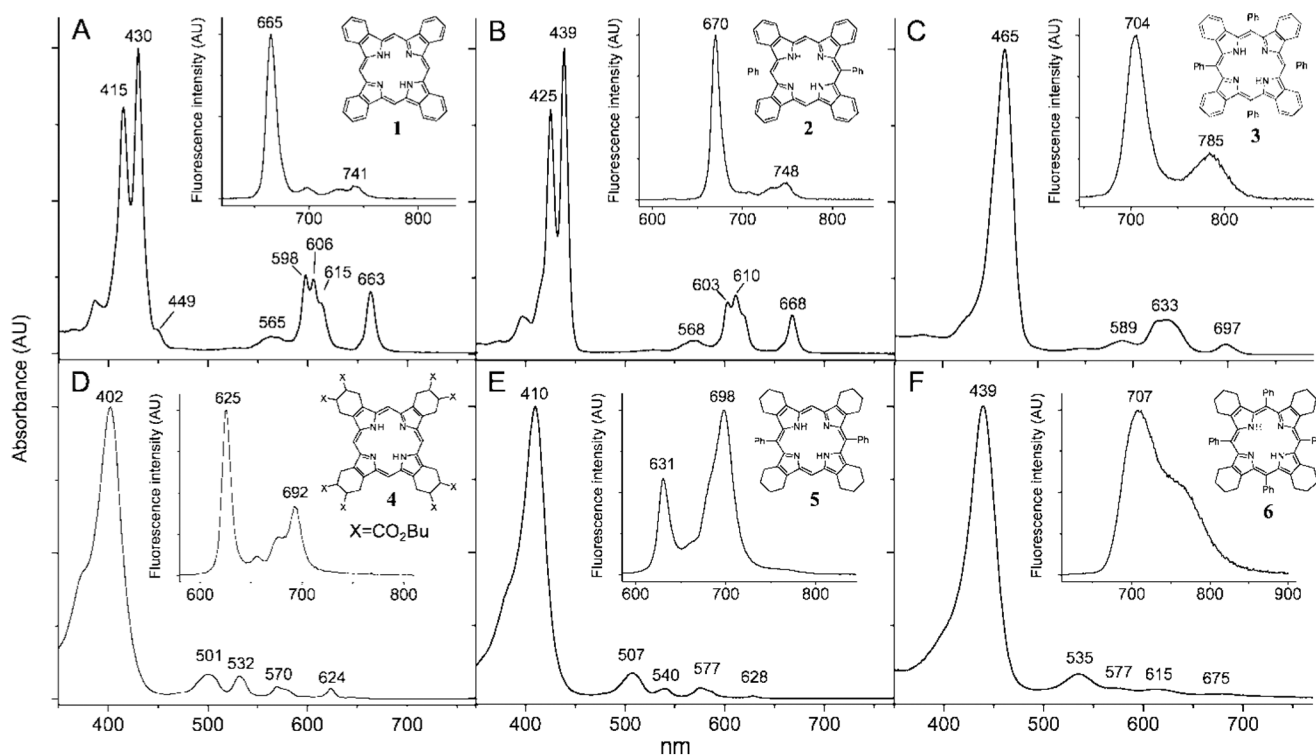
Support of the grants EB007279 and HL081273 from the NIH USA and RFBR-04-03-32650 and RFBR-07-03-01121 from the Russian Foundation of Basic Research is gratefully acknowledged. We thank Dr. Thomas Troxler (Penn RLBL, NIH P41-RR001348) for assistance with fluorescence lifetime measurements, Drs. K. Lutsenko (INEOS RAN) and Patrick Carroll (Penn) for X-ray structure determination and Prof. Craig Medforth (University of New Mexico) for providing structural data on 5,15-diaryl- $\beta$ -octaalkylporphyrins. SAV thanks Prof. Robin M. Hochstrasser for invaluable discussions.

## References and Notes

1. a Ehrenberg B, Malik Z, Nitzan Y, Ladan H, Johnson FM, Hemmi G, Sessler JL. *Lasers Med. Sci* 1993;8:197. b Gross E, Ehrenberg B, Johnson FM. *Photochem. Photobiol* 1993;57:808. [PubMed: 8337252] c Lavi A, Johnson FM, Ehrenberg B. *Chem. Phys. Lett* 1994;231:144. d Yasuike M, Yamaoka T, Ohno O, Sakuragi M, Ichimura K. *Inorg. Chim. Acta* 1991;184:191. e Friedberg JS, Skema C, Baum ED, Burdick J, Vinogradov SA, Wilson DF, Horan AD, Nachamkin I. *J. Antimicrob. Chemother* 2001;48:105. [PubMed: 11418518] f Kepczynski M, Pandian RP, Smith KM, Ehrenberg B. *Photochem. Photobiol* 2002;76:127. [PubMed: 12194207] g Ongayi O, Gottumukkala V, Fronczek FR, Vicente MGH. *Bioorg. Med. Chem. Lett* 2005;15:1665. [PubMed: 15745818] h Gottumukkala V, Ongayi O, Baker DG, Lomax LG, Vicente MGH. *Bioorg. Med. Chem* 2006;14:1871. [PubMed: 16298134]
2. a Vinogradov SA, Wilson DF. *J. Chem. Soc. Perkin Trans* 1995;2:103–111. b Vinogradov SA, Lo L-W, Jenkins WT, Evans SM, Koch C, Wilson DF. *Biophys. J* 1996;70:1609. [PubMed: 8785320] c Finikova OS, Galkin A, Rozhkov VV, Cordero M, Hägerhäll C, Vinogradov SA. *J. Am. Chem. Soc* 2003;125:4882. [PubMed: 12696908] d Rietveld IB, Kim E, Vinogradov SA. *Tetrahedron* 2003;59:3821. e Apreleva SV, Wilson DF, Vinogradov SA. *Appl. Opt* 2006;45:8547. [PubMed: 17086268] f Wilson DF, Lee WMF, Makonnen S, Finikova O, Apreleva S, Vinogradov SA. *J. Appl. Physiol* 2006;101:1648. [PubMed: 16888050] g Finikova OS, Troxler T, Senes A, DeGrado WF, Hochstrasser RM, Vinogradov SA. *J. Phys. Chem. A* 2007;111:6977. [PubMed: 17608457] h Mik EG, Johannes T, Ince C. *Amer J. Physiol. Renal Physiol* 2008;294:F676. [PubMed: 18184739]
3. a Balushev S, Yakutkin V, Miteva T, Avlasevich Y, Chernov S, Aleshchenkov S, Nelles G, Cheprakov A, Yasuda A, Mullen K, Wegner G. *Angew. Chem., Int. Ed* 2007;46:7693. b Balushev S, Yakutkin V, Wegner G, Miteva T, Nelles G, Yasuda A, Chernov S, Aleshchenkov S, Cheprakov A. *App. Phys. Lett* 2007;90:181103. c Balushev S, Yakutkin V, Miteva T, Wegner G, Roberts T, Nelles G, Yasuda A, Chernov S, Aleshchenkov S, Cheprakov A. *New J. Phys* 2008;10:1.
4. a Hanack M, Ziplies T. *J. Am. Chem. Soc* 1985;107:6127. b Guha S, Kang K, Porter P, Roach JF, Remy DE, Aranda FJ, Rao DVGLN. *Opt. Lett* 1992;17:264. c Chen PL, Tomov IV, Dvornikov AS, Nakashima M, Roach JF, Alabran DM, Rentzepis PM. *J. Phys. Chem* 1996;100:17507. d Brunel M, Chaput F, Vinogradov SA, Campagne B, Canva M, Boilot JP, Brun A. *Chem. Phys* 1997;218:301. e Plagemann B, Renge I, Renn A, Wild UP. *J. Phys. Chem. A* 1998;102:1725. f Borek C, Hanson K, Djurovich PI, Thompson ME, Aznavour K, Bau R, Sun YR, Forrest SR, Brooks J, Michalski L, Brown J. *Angew. Chem., Int. Ed* 2007;46:1109.
5. a Phillips TE, Hoffman BM. *J. Am. Chem. Soc* 1977;99:7734. b Martinsen J, Pace LJ, Phillips TE, Hoffman BM, Ibers JA. *J. Am. Chem. Soc* 1982;104:83. c Liou K, Ogawa MY, Newcomb TP, Quirion G, Lee MH, Poirier M, Halperin WP, Hoffman BM, Ibers JA. *Inorg. Chem* 1989;28:3889. d Liou KY, Newcomb TP, Heagy MD, Thompson JA, Heuer WB, Musselman RL, Jacobsen CS, Hoffman BM, Ibers JA. *Inorg. Chem* 1992;31:4517. e Kobayashi N, Nevin WA, Mizunuma S, Awaji H, Yamaguchi M. *Chem. Phys. Lett* 1993;205:51. f Murata K, Liou KK, Thompson JA, McGhee EM, Rende DE, Ellis DE, Musselman RL, Hoffman BM, Ibers JA. *Inorg. Chem* 1997;36:3363. [PubMed: 11670003] g Aramaki S, Sakai Y, Ono N. *Appl. Phys. Lett* 2004;84:2085–2087. h Shea PB, Johnson AR, Ono N, Kanicki J. *IEEE Trans. Electron Devices* 2005;52:1497.
6. a Gouterman M. *J. Mol. Spectrosc* 1961;6:138. b Bajema L, Gouterman M, Rose C. *J. Mol. Spectrosc* 1971;39:421. c Edwards L, Gouterman M, Rose CB. *J. Am. Chem. Soc* 1976;98:7638. [PubMed:

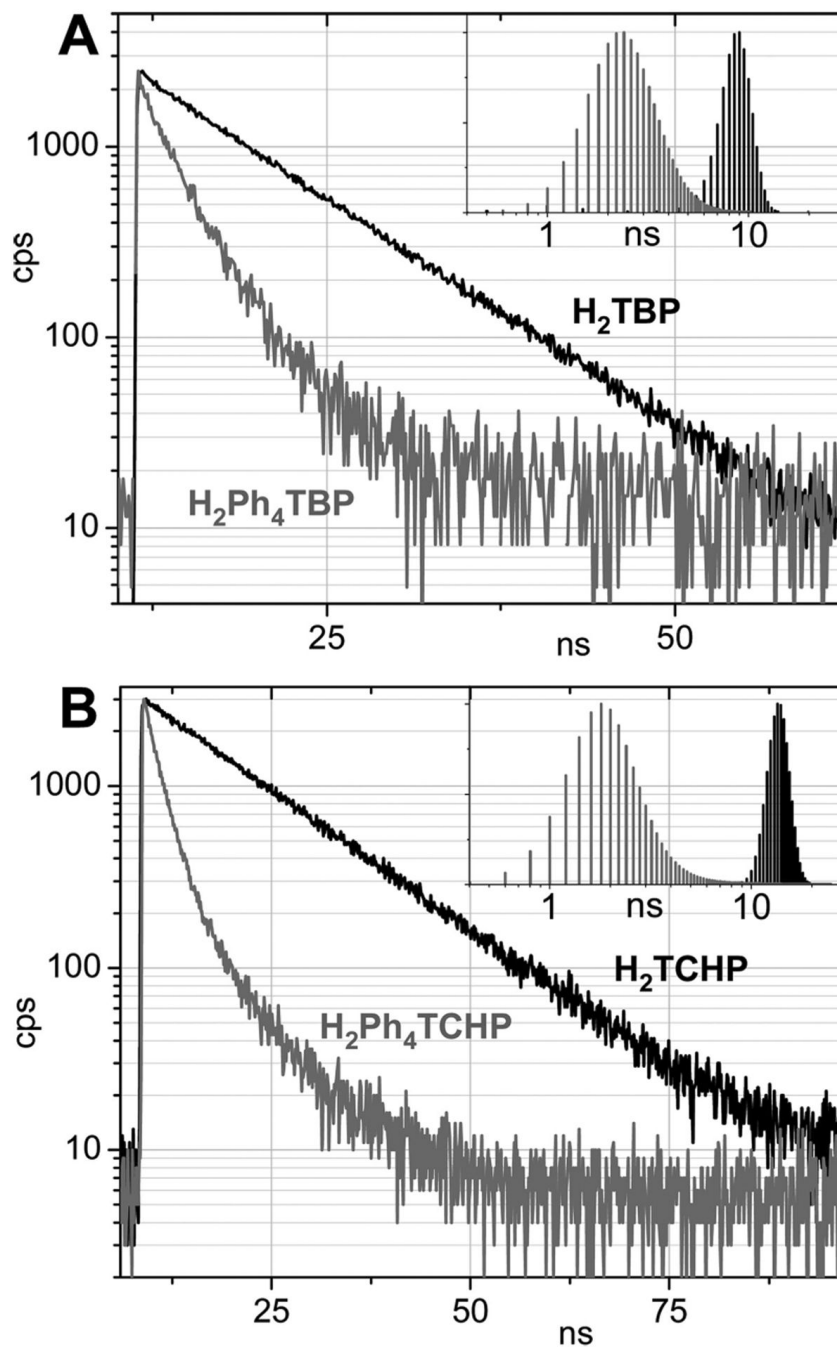
- 993497] d Aartsma TJ, Gouterman M, Jochum C, Kwiram AL, Pepich BV, Williams LD. *J. Am. Chem. Soc* 1982;104:6278.
7. a Sevchenko AN, Solovov KN, Shkirman SF, Kachura TF. *Doklady Akademii Nauk SSSR (Russ)* 1965;161:1313. b Tsvirko MP, Sapunov VV, Soloviyev KN. *Optics Spectrosc.(Russ)* 1973;34:1094.
8. a Vogler A, Kunkely H. *Inorg. Chim. Acta* 1980;44:L211. b Vogler A, Kunkely H, Rethwisch B. *Inorg. Chim. Acta* 1980;46:101. c Koehorst RBM, Kleibeuker JF, Tjeerd JS, de Bie DA, Geursten B, Henrie RN, van der Plas HC. *J. Chem. Soc* 1981:1005. d Ehrenberg B, Johnson FM. *Spectrochim. Acta* 1990;46a:1521. e Madoka Y, Tsiguo Y, Osami O, Kunihiro I, Hisayuki M, Masako S. *Inorg. Chim. Acta* 1991;185:39.
9. a Kobayashi N, Konami H. *J. Porphyrins Phthalocyanines* 2001;5:233. b Rosa A, Ricciardi G, Baerends EJ, van Gisbergen SJA. *J. Phys. Chem. A* 2001;105:3311. c Nguyen KA, Pachter R. *J. Chem. Phys* 2001;114:10757. d Zamyatin AV, Soldatova AV, Rodgers MAJ. *Inorg. Chim. Acta* 2007;360:857.
10. Rogers JE, Nguyen KA, Hufnagle DC, McLean DG, Su WJ, Gossett KM, Burke AR, Vinogradov SA, Pachter R, Fleitz PA. *J. Phys. Chem. A* 2003;107:11331.
11. Shelnutt JA, Song XZ, Ma JG, Jia SL, Jentzen W, Medforth CJ. *Chem. Soc. Rev* 1998;27:31.
12. a Medforth CJ, Dolores Berber M, Smith KM, Shelnutt JA. *Tetrahedron Lett* 1990;31:3719. b Shelnutt JA, Medforth CJ, Berber MD, Barkigia KM, Smith KM. *J. Am. Chem. Soc* 1991;113:4077. c Charlesworth P, Truscott TG, Kessel D, Medforth CJ, Smith KM. *J. Chem. Soc. Faraday Trans* 1994;90:1073. d Ravikanth M, Reddy D, Chandrashekar TK. *J. Photochem. Photobiol* 1993;72:61. e Reddy D, Chandrashekar TK, Vanwilligen H. *Chem. Phys. Lett* 1993;202:120. f Wertsching AK, Koch AS, DiMagno SG. *J. Am. Chem. Soc* 2001;123:3932. [PubMed: 11457143] g Ryeng H, Ghosh A. *J. Am. Chem. Soc* 2002;124:8099. [PubMed: 12095355] h Haddad RE, Gazeau S, Pecaut J, Marchon JC, Medforth CJ, Shelnutt JA. *J. Am. Chem. Soc* 2003;125:1253. [PubMed: 12553827]
13. a Gentemann S, Medforth CJ, Forsyth TP, Nurco DJ, Smith KM, Fajer J, Holten D. *J. Am. Chem. Soc* 1994;116:7363. b Gentemann S, Medforth CJ, Ema T, Nelson NY, Smith KM, Fajer J, Holten D. *Chem. Phys. Lett* 1995;245:441. c Drain CM, Kirmaier C, Medforth CJ, Nurco J, Smith KM, Holten D. *J. Phys. Chem* 1996;100:11984. d Gentemann S, Nelson NY, Jaquinod L, Nurco DJ, Leung SH, Medforth CJ, Smith KM, Fajer J, Holten D. *J. Phys. Chem. B* 1997;101:1247. e Drain CM, Gentemann S, Roberts JA, Nelson NY, Medforth CJ, Jia SL, Simpson MC, Smith KM, Fajer J, Shelnutt JA, Holten D. *J. Am. Chem. Soc* 1998;120:3781. f Retsek JL, Gentemann S, Medforth CJ, Smith KM, Chirvony VS, Fajer J, Holten D. *J. Phys. Chem. B* 2000;104:6690. g Chirvony VS, van Hoek A, Galievsky VA, Sazanovich IV, Schaafsma TJ, Holten D. *J. Phys. Chem. B* 2000;104:9909. h Sazanovich IV, Galievsky VA, van Hoek A, Schaafsma TJ, Malinovskii VL, Holten D, Chirvony VS. *J. Phys. Chem. B* 2001;105:7818.
14. a Aaviksoo J, Frieberg A, Savikhin S, Stelmakh GF, Tsvirko MP. *Chem. Phys. Lett* 1984;111:275. b Ehrenberg B, Johnson FM. *Spectrochim. Acta* 1990;46a:1521. c Yasuike M, Koseki K, Yamaoka T, Ichimura K, Sakuragi M, Ohno O. *Inorg. Chim. Acta* 1991;183:9.
15. a Roitman L, Ehrenberg B, Kobayashi N. *J. Photochem. Photobiol. A Chem* 1994;77:23. b Vinogradov SA, Wilson DF. *Adv. Exp. Med. Biol* 1997;411:597. [PubMed: 9269478] c Rozhkov VV, Khajehpour M, Vinogradov SA. *Inorg. Chem* 2003;42:4253. [PubMed: 12844293]
16. Cheng RJ, Chen YR, Wang SL, Cheng CY. *Polyhedron* 1993;12:1353.
17. A number of X-ray structures of tetrabenzoporphyrin-cations was determined by Ibers et al.5b-d
18. a Finikova O, Cheprakov A, Beletskaya I, Vinogradov S. *Chem. Commun* 2001:261. b Finikova OS, Cheprakov AV, Beletskaya IP, Carroll PJ, Vinogradov SA. *J. Org. Chem* 2004;69:522. [PubMed: 14725469] c Finikova OS, Cheprakov AV, Carroll PJ, Vinogradov SA. *J. Org. Chem* 2003;68:7517. [PubMed: 12968910] d Finikova OS, Aleshchenkov SE, Brinas RP, Cheprakov AV, Carroll PJ, Vinogradov SA. *J. Org. Chem* 2005;70:4617. [PubMed: 15932297] e Finikova OS, Cheprakov AV, Vinogradov SA. *J. Org. Chem* 2005;70:9562. [PubMed: 16268634] f Filatov MA, Cheprakov AV, Beletskaya IP. *Eur. J. Org. Chem* 2007:3468. g Filatov MA, Lebedev AY, Vinogradov SA, Cheprakov AV. *J. Org. Chem* 2008;73:4175. [PubMed: 18452337]
19. Senge, MO. Ch. 6 in *The Porphyrin Handbook*. Kadish, KM.; Smith, KM.; Guilard, R., editors. Academic Press; 2000, and references therein.; b Senge MO. *Chem. Commun* 2006:243.
20. a Avilov IV, Zenkevich EI, Sagun EI, Filatov IV. *J. Phys. Chem. A* 2004;108:5684. b Chirvony VS, Avilov IV, Panarin AY, Malinovskii VL, Galievsky VA. *Chem. Phys. Lett* 2007;434:116.

21. a Knyukshto VN, Sagun EI, Shul'ga AM, Bachilo SM, Starukhin DA, Zen'kevich EI. *Opt. Spectrosc* 2001;90:67. b Knyukshto VN, Shul'ga AM, Sagun EI, Zen'kevich EI. *Opt. Spectrosc* 2002;92:53. c Knyukshto VN, Shul'ga AM, Sagun EI, Zen'kevich EI. *Opt. Spectrosc* 2006;100:590–601.
22. a Jentzen W, Song X-Z, Shelnett JA. *J. Phys. Chem. B* 1997;101:1684. b Jentzen W, Ma JG, Shelnett JA. *Biophys. J* 1998;74:753. [PubMed: 9533688]
23. Medforth CJ, Senge MO, Smith KM, Sparks LD, Shelnett JA. *J. Am. Chem. Soc* 1992;114:9859.
24. Rosa A, Ricciardi G, Baerends EJ. *J. Phys. Chem. A* 2006;110:5180. [PubMed: 16610842]
25. Seybold PG, Gouterman M. *J. Mol. Spectrosc* 1969;31:1.
26. Gradyushko AT, Tsvirko MP. *Optics Spectrosc. (Russ)* 1971;31:291.
27. In photochemical literature, *funnels* or *conical intersections* (as opposed to *avoided crossings*) usually refer to the points in which the ground and excited state potential energy surfaces touch, resulting in sub-picosecond non-radiative relaxation (for review see Garavelli M. *Theor. Chem. Acc* 2006;116:87.). In the aforementioned model, 13 *funnels* more broadly refer to local minima on the  $S_1$  potential energy surface, in which the  $S_1-S_0$  gaps are small and internal conversion is enhanced in accordance with the energy gap law.
28. Finikova OS, Cheprakov AV, Carroll PJ, Dalosto S, Vinogradov SA. *Inorg. Chem* 2002;41:6944. [PubMed: 12495329]
29. Senge MO, Forsyth T, Nguyen LT, Smith KM. *Angew. Chem., Int. Ed* 1994;33:2485.
30. a Livesey AK, Brochon JC. *Biophys. J* 1987;52:693. b Vinogradov SA, Wilson DF. *Appl. Spectrosc* 2000;54:849.
31. Yasuike M, Yamaoka T, Ohno O, Kunihiro I, Morii H, Sakuragi M. *Inorg. Chim. Acta* 1991;185:39. The reported absorption spectrum and the fluorescent properties, although in general consistent with our data, indicate that their samples contained other *meso*-aryl TBP's.
32. Barret PA, Linstead RP, Rundall FG, Tuey GAP. *J. Chem. Soc* 1940:1079.
33. Senge MO, Medforth CJ, Forsyth TP, Lee DA, Olmstead MM, Jentzen W, Pandey RK, Shelnett JA, Smith KM. *Inorg. Chem* 1997;36:1149. [PubMed: 11669682]
34. Senge MO, Bischoff I. *Heterocycles* 2005;65:879.
35. Giraud-Roux M, Proni G, Nakanishi K, Berova N. *Heterocycles* 2003;61:417.
36. Yamada H, Kushibe K, Okujima T, Uno H, Ono N. *Chem. Commun* 2006:383.
37. Eastwood D, Gouterman M. *J. Mol. Spectrosc* 1970;35:359.
38. Antipas A, Gouterman M. *J. Am. Chem. Soc* 1983;105:4896.
39. Based on the experimental and calculated structures of other metal complexes of O ETPP (e.g. Zn, Ni, Cu), 40 PdOETPP is considered to possess saddled geometry.
40. a Barkigia KM, Berber MD, Fajer J, Medforth CJ, Renner MW, Smith KM. *J. Am. Chem. Soc* 1990;112:8851. b Barkigia KM, Renner MW, Furenlid LR, Medforth CJ, Smith KM, Fajer J. *J. Am. Chem. Soc* 1993;115:3627. c Renner MW, Barkigia KM, Zhang Y, Medforth CJ, Smith KM, Fajer J. *J. Am. Chem. Soc* 1994;116:8582.
41. Stolzenberg AM, Schussel LJ, Summers JS, Foxman BM, Petersen JL. *Inorg. Chem* 1992;31:1678.
42. a Sessler JL, Johnson MR, Creager SE, Fettinger JC, Ibers JA. *J. Am. Chem. Soc* 1990;112:9310. b Stulz E, Scott SM, Ng YF, Bond AD, Teat SJ, Darling SL, Feeder N, Sanders JKM. *Inorg. Chem* 2003;42:6564. [PubMed: 14514334]
43. Minaev B, Ågren H. *Chem. Phys* 2005;315:215.
44. Fleischer EB, Webb LE, Miller CK. *J. Am. Chem. Soc* 1964;86:2342.
45. Lipstman S, Goldberg I. *Acta Crystallogr. C: Cryst. Struct. Commun* 2008;64:M53–M57.



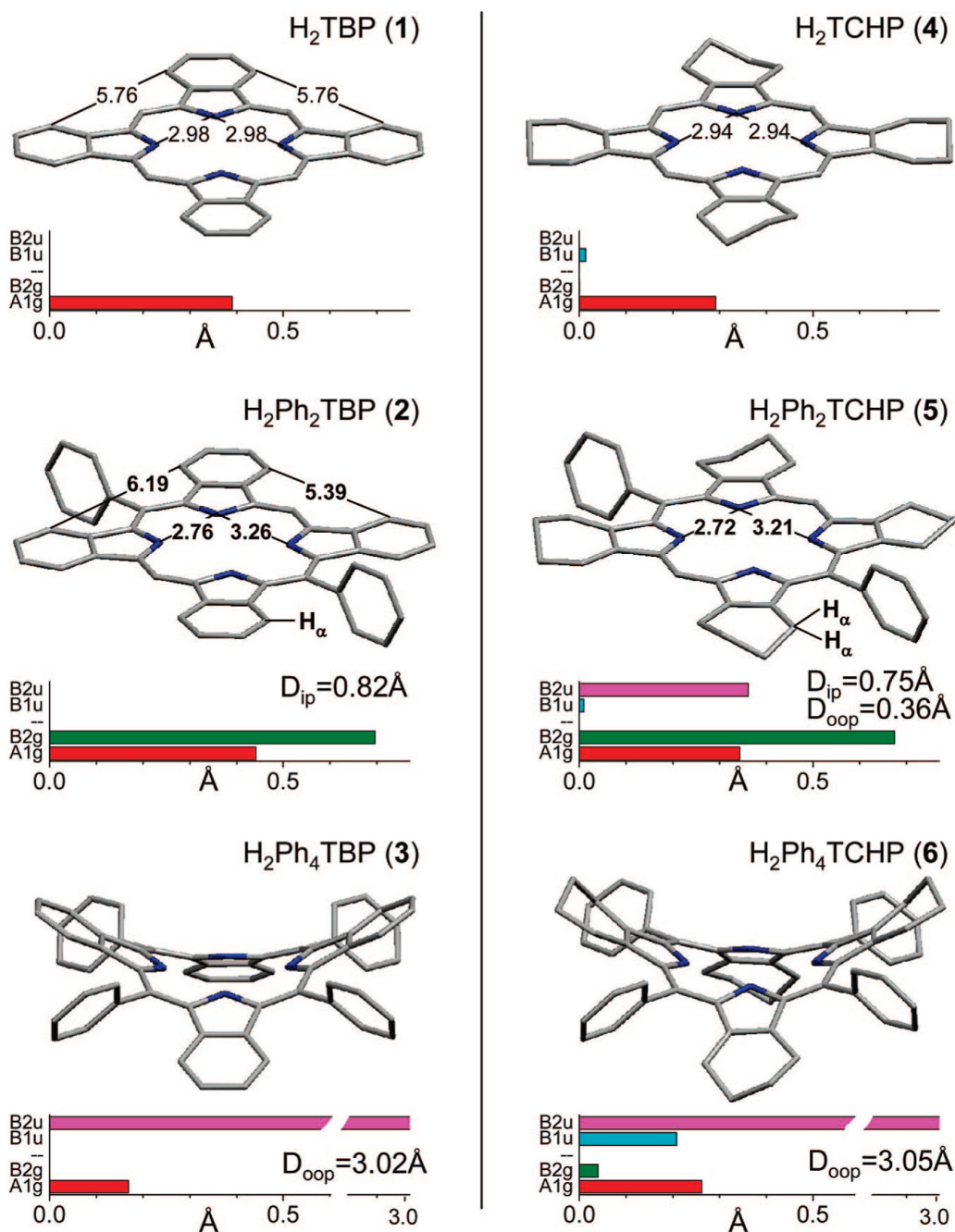
**Figure 1.**

Absorption and fluorescence (insets) spectra of H<sub>2</sub>TBP (**1**, A) (H<sub>2</sub>TBP was first dissolved in pyridine, and a drop of this solution was added to toluene.), H<sub>2</sub>Ph<sub>2</sub>TBP (**2**, B), H<sub>2</sub>Ph<sub>4</sub>TBP (**3**, C) and H<sub>2</sub>TCHP(CO<sub>2</sub>Bu)<sub>8</sub> (**4**, D), H<sub>2</sub>Ph<sub>2</sub>TCHP (**5**, E) and H<sub>2</sub>Ph<sub>4</sub>TCHP (**6**, F) (Small amount of TMEDA was added to prevent dication formation.) in toluene at 295 K.



**Figure 2.** Fluorescence decays for H<sub>2</sub>TBP (1), H<sub>2</sub>Ph<sub>4</sub>TBP (3) (A) and H<sub>2</sub>TBP (4) and H<sub>2</sub>Ph<sub>4</sub>TBP (6) (B) in toluene at 296 K and the underlying lifetime distributions, recovered by the Maximum Entropy Method.



**Figure 3.**

Computed structures (DFT B3LYP/6-31G(d)) of H<sub>2</sub>Ph<sub>n</sub>TBP's (left column) and Ph<sub>n</sub>TCHP's (right column) ( $n = 0, 2, 4$ ). Distances are in Å. Main distortion modes, recovered by the NSD analysis,<sup>22</sup> are shown by the bar graphs. In-plane distortions: A<sub>1g</sub>, red; B<sub>2g</sub>, green. Out-of-plane distortions: B<sub>1u</sub> (ruffling), cyan; B<sub>2u</sub> (saddling), magenta. (For complete list of modes see Supporting Information, V). D<sub>oop</sub> and D<sub>ip</sub> designate total mean-square out-of-plane and in-plane displacements, respectively.

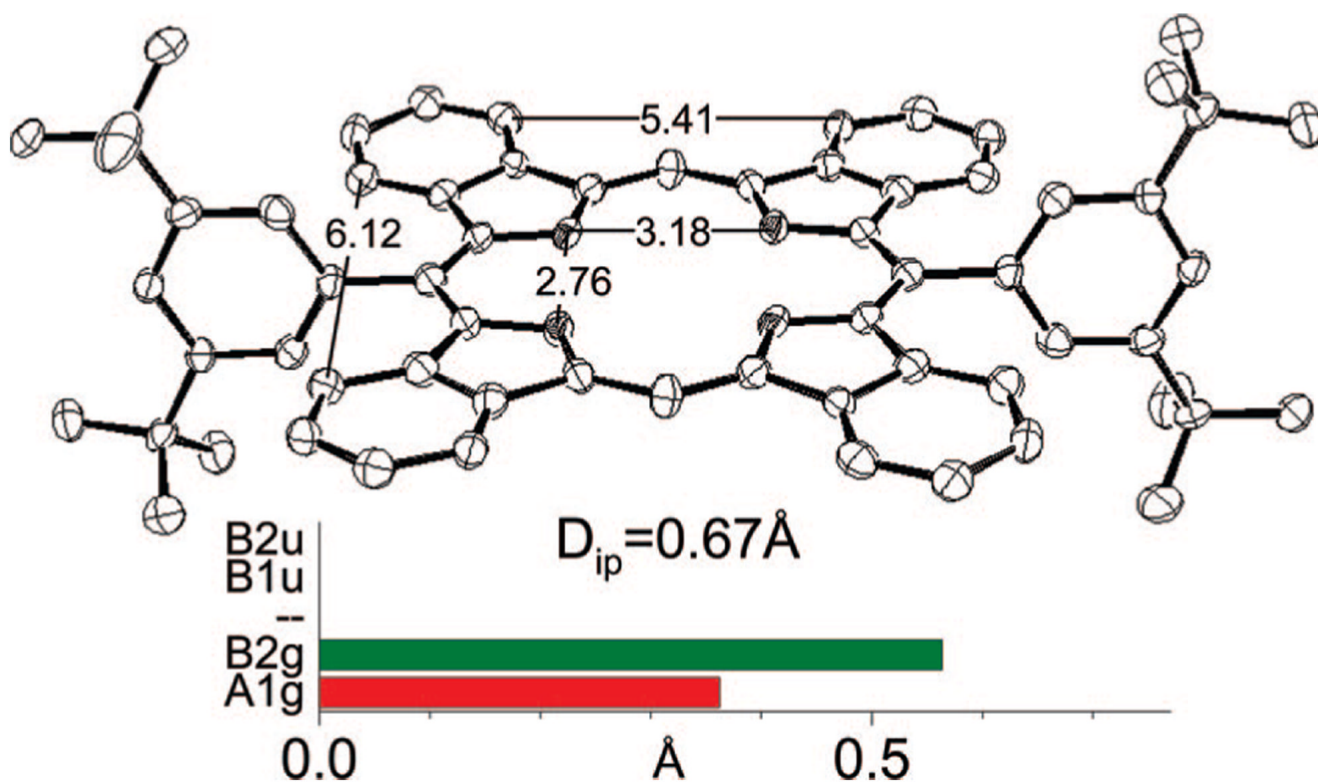


**Figure 4.** X-ray crystal structure of  $H_2Ar_2TBP$  ( $Ar = 3,5-tBu_2C_6H_3$ ) and its NSD analysis. Distances are in Å. Hydrogen atoms are omitted for clarity.

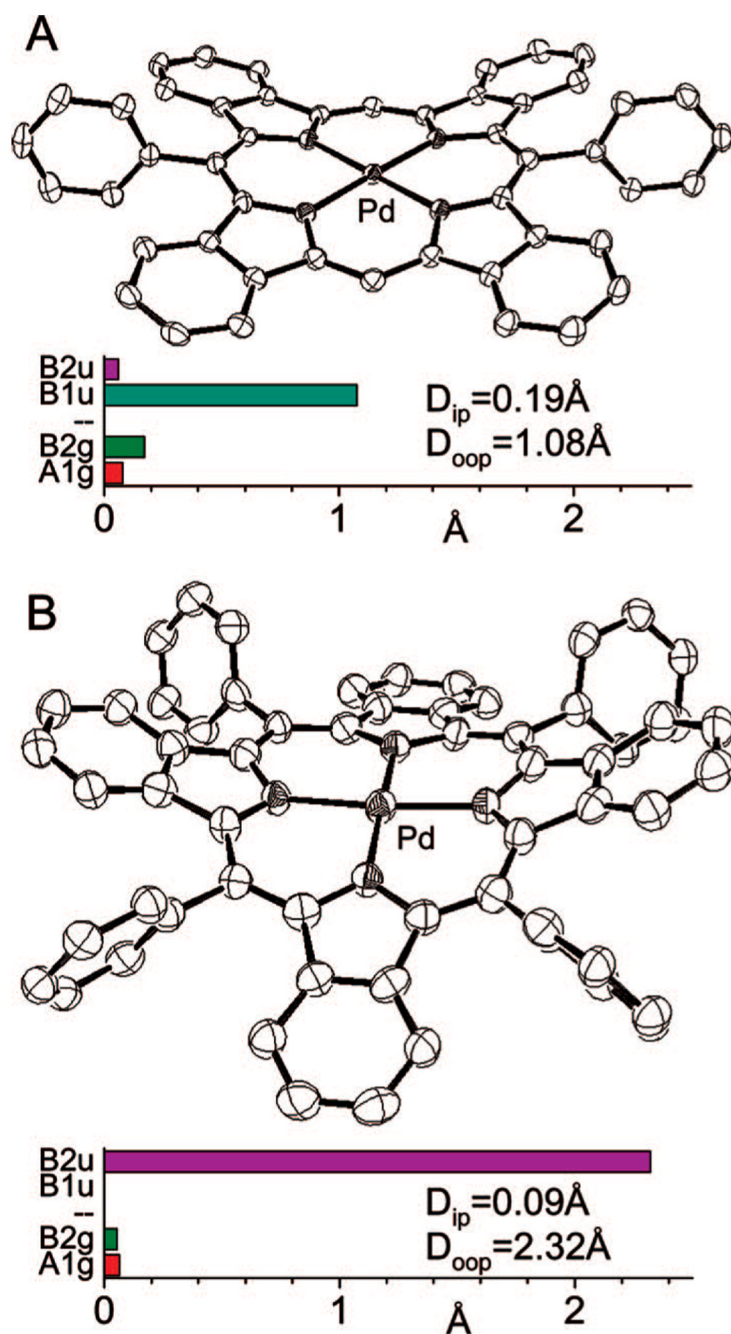


**Figure 5.** X-ray crystal structures of PdPh<sub>2</sub>TBP (**Pd-2**) (A) and PdAr<sub>4</sub>TBP (Ar = 3,5-(BuO<sub>2</sub>C)<sub>2</sub>C<sub>6</sub>H<sub>3</sub>) (B) and their NSD analyses. Hydrogen atoms and substituents in the *meso*-aryl rings in PdAr<sub>4</sub>TBP (B) are not shown for clarity (see Supporting Information, IV for complete structure).

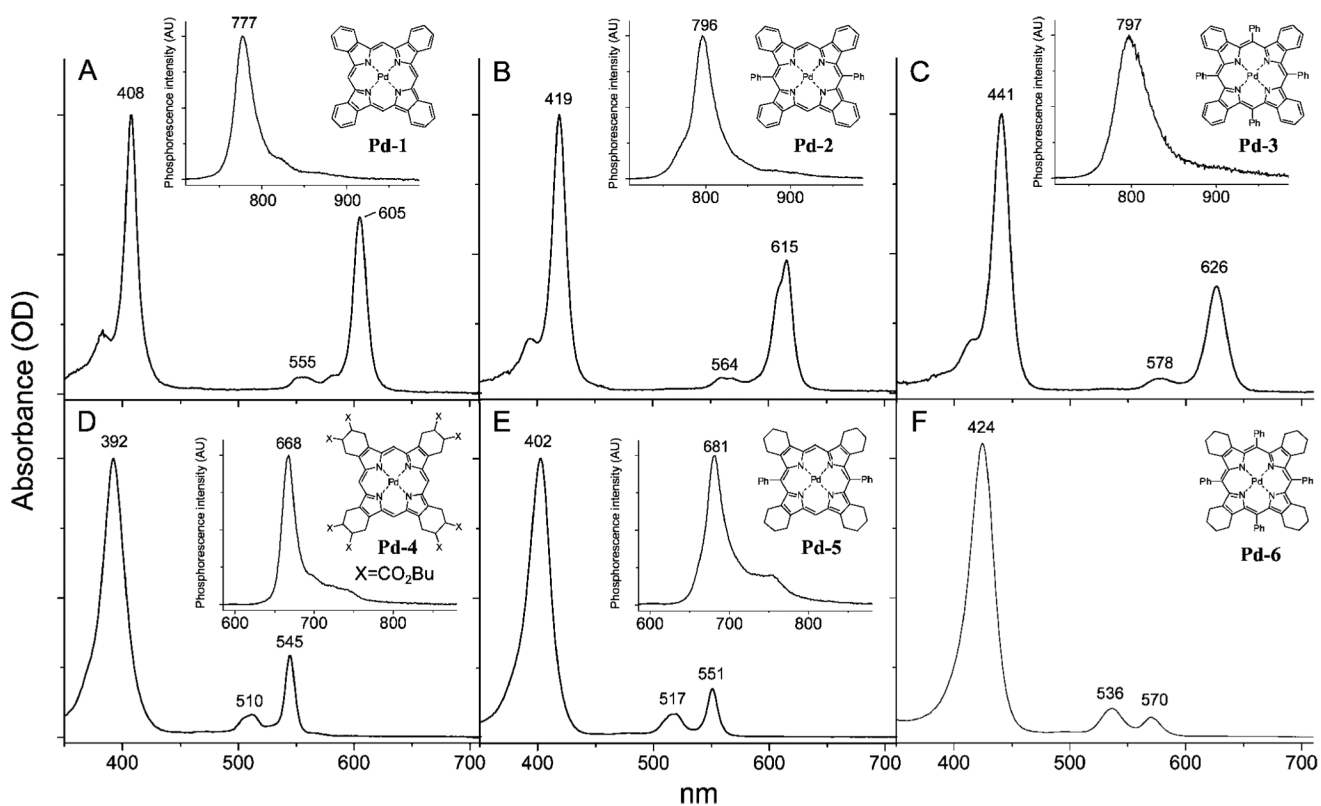
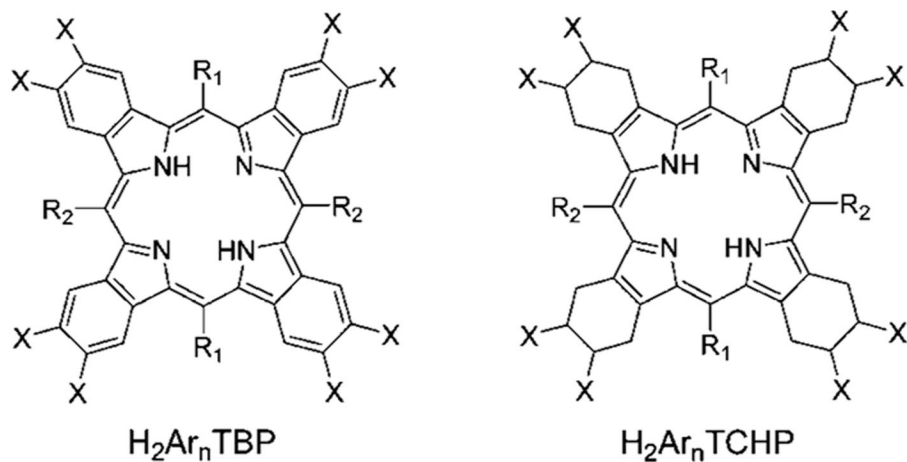


**Figure 6.** Absorption and phosphorescence (insets) spectra of PdTBP (**Pd-1**, A), PdPh<sub>2</sub>TBP (**Pd-2**, B), PdPh<sub>4</sub>TBP (**Pd-3**, C) and PdTCHP(CO<sub>2</sub>Bu)<sub>8</sub> (**Pd-4**, D), PdPh<sub>2</sub>TCHP (**Pd-5a**, E) and PdPh<sub>4</sub>TCHP (**6**, F) in DMA at 295 K.



**1:** R<sub>1</sub>=R<sub>2</sub>=H, X=H

**1a:** X=CO<sub>2</sub>Bu

**2:** R<sub>1</sub>=Ph, R<sub>2</sub>=H, X=H

**2a:** R<sub>1</sub>=4-MeO<sub>2</sub>C-C<sub>6</sub>H<sub>4</sub>

**3:** R<sub>1</sub>=R<sub>2</sub>=Ph, X=H

**3a:** R<sub>1</sub>=R<sub>2</sub>=4-MeO<sub>2</sub>C-C<sub>6</sub>H<sub>4</sub>

**3c:** R<sub>1</sub>=R<sub>2</sub>=3,5-(BuO<sub>2</sub>C)<sub>2</sub>-C<sub>6</sub>H<sub>3</sub>

**4:** R<sub>1</sub>=R<sub>2</sub>=H, X=CO<sub>2</sub>Bu

**5:** R<sub>1</sub>=Ph, R<sub>2</sub>=H, X=H

**5a:** R<sub>1</sub>=4-MeO<sub>2</sub>C-C<sub>6</sub>H<sub>4</sub>

**6:** R<sub>1</sub>=R<sub>2</sub>=Ph, X=H

The corresponding Pd complexes are abbreviated as **Pd-1**, **Pd-2** etc.

CHART 1.

**TABLE 1**  
Photophysical Properties of Free-Base Porphyrins H<sub>2</sub>Ar<sub>n</sub>TBP and H<sub>2</sub>Ar<sub>n</sub>TCHP  
(*n*) = 0, 2, 4) in Toluene at 295 K and in Dimethylacetamide (DMA, Noted)<sup>a</sup>

free-base porphyrin	fluorescence $\lambda_{\text{max}}$ ( $\lambda_{\text{ex}}$ ), nm	Stokes shift (cm <sup>-1</sup> )	$\phi_{\text{f}}$ <sup>b</sup>	$\tau_{\text{f}}$ (ns) <sup>c</sup>
TBP				
<b>1</b>	665, 741 (571)	45.4	0.35	9.8
<b>1</b> (in DMA)	663, 740 (571)	45.6	0.47	—
<b>2</b>	670, 746 (571)	44.7	0.34	10.3
<b>2</b> (in DMA)	668, 744 (517)	45.0	0.41	—
<b>2a</b>	668, 744 (517)	45.0	—	9.6
<b>3</b>	705, 786 (635)	162.8	0.03	2.8 <sup>c</sup>
<b>3</b> (in DMA)	707, 791 (635)	223.5	0.02	—
<b>3a</b>	712, 792 (594)	220.4	0.03	2.9 <sup>c</sup>
TCHP				
<b>4</b>	625, 692 (531)	25.6	0.14	14.1
<b>5</b>	631, 698 (507)	75.7	0.08	11.8
<b>6</b>	707 (535)	670	0.01	2.6 <sup>c</sup>
<b>6</b> (in DMA)	720 (635)	882	<0.01	—

<sup>a</sup> A drop of H<sub>2</sub>TBP solution in pyridine was added to toluene.

<sup>b</sup> Quantum yields were measured relative to the fluorescence of H<sub>2</sub>TPP in deoxygenated C<sub>6</sub>H<sub>6</sub> ( $\phi_{\text{f}} = 0.11$  in deoxygenated benzene).<sup>25</sup> Error in determination of yields is no more than 10%. Purging samples with Ar was shown to increase the fluorescence quantum yields by no more than 5% both in toluene and DMA.

<sup>c</sup> Inhomogeneous multiexponential decays with broad lifetime distributions were detected. Average lifetime value is reported in the Table 1.

**TABLE 2**  
Deactivation Rate Constants for S<sub>1</sub> State of Free-Base Porphyrins H<sub>2</sub>Ar<sub>*n*</sub>TBP and H<sub>2</sub>Ar<sub>*n*</sub>TCHP (*n* = 0, 2, 4) in Toluene at 295 K

compound	$k = 1/\tau_n$ (s <sup>-1</sup> )	$k_r$ (s <sup>-1</sup> ) <sup>a</sup>	$k_{nr}$ (s <sup>-1</sup> ) <sup>b</sup>
TBP			
H <sub>2</sub> TBP (1)	$1.02 \times 10^8$	$3.57 \times 10^7$	$6.63 \times 10^7$
H <sub>2</sub> Ph <sub>2</sub> TBP (2)	$9.71 \times 10^7$	$3.30 \times 10^7$	$6.41 \times 10^7$
H <sub>2</sub> Ph <sub>4</sub> TBP (3)	$3.57 \times 10^8$	$1.07 \times 10^7$	$3.46 \times 10^8$
TCHP			
H <sub>2</sub> TCHP (4)	$7.09 \times 10^7$	$9.93 \times 10^6$	$6.10 \times 10^7$
H <sub>2</sub> Ph <sub>2</sub> TCHP (5)	$8.47 \times 10^7$	$6.78 \times 10^6$	$7.80 \times 10^7$
H <sub>2</sub> Ph <sub>4</sub> TCHP (6)	$3.85 \times 10^8$	$3.85 \times 10^6$	$3.81 \times 10^8$

<sup>a</sup>  $k_r$  radiative decay rate constant, calculated as  $k_r = \phi_f k$ , where  $\phi_f$  is the fluorescence quantum yield.

<sup>b</sup>  $k_{nr}$ , nonradiative decay rate constant ( $k_{nr} = k_{ic} + k_{isc}$ ), calculated as  $k_r = k - k_{nr}$ .

**TABLE 3**  
Photophysical Properties of PdAr<sub>n</sub>TBP and PdAr<sub>n</sub>TCHP (*n* = 0, 2, 4) in Deoxygenated DMA at 295 K

Pd porphyrin	phosphorescence $\lambda_{\text{max}}$ ( $\lambda_{\text{ex}}$ ), nm	$\phi_{\text{phos}}^a$	$\tau_{\text{phos}}$ ( $\mu\text{s}$ ) <sup>b</sup>
	TBP		
<b>Pd-1</b>	777 (605)	0.13	399
<b>Pd-1a</b>	770 (615)	0.35	496
<b>Pd-2</b>	796 (615)	0.15	423
<b>Pd-3</b>	797 (626)	0.08	258
	TCHP		
<b>Pd-4</b>	668 (545)	0.45	1118
<b>Pd-5</b>	681 (550)	0.02	97
<b>Pd-6</b>	—	— <sup>c</sup>	— <sup>c</sup>

<sup>a</sup> Measured relative to the fluorescence of H<sub>2</sub>TPP in deoxygenated C<sub>6</sub>H<sub>6</sub> ( $\phi_{\text{fl}} = 0.11$ ).<sup>25</sup> Error in determination of yields is no more than 10%.

<sup>b</sup> Phosphorescence decays were nearly ideally single-exponential, as revealed by the Maximum Entropy analysis.

<sup>c</sup> No signal could be detected.



**TABLE 4**  
Deactivation Rate Constants for T<sub>1</sub> state of PdAr<sub>n</sub>TBP and PdAr<sub>n</sub>TCHP (*n* = 0, 2, 4) in Deoxygenated DMA at 295 K

compound	$k = 1/\tau_{\text{phos}} \text{ (s}^{-1}\text{)}$	$k_{\text{r}} \text{ (s}^{-1}\text{)}^a$	$k_{\text{nr}} \text{ (s}^{-1}\text{)}^b$
TBP			
PdTBP ( <b>Pd-1</b> )	$2.51 \times 10^3$	$3.26 \times 10^2$	$2.18 \times 10^3$
<b>Pd-1a</b>	$2.02 \times 10^3$	$7.06 \times 10^2$	$1.31 \times 10^3$
PdPh <sub>2</sub> TBP ( <b>Pd-2</b> )	$2.36 \times 10^3$	$3.55 \times 10^2$	$2.00 \times 10^3$
PdPh <sub>4</sub> TBP ( <b>Pd-3</b> )	$3.88 \times 10^3$	$3.10 \times 10^2$	$3.57 \times 10^3$
TCHP			
PdTCHP ( <b>4</b> )	$8.94 \times 10^2$	$4.02 \times 10^2$	$4.92 \times 10^2$
PdPh <sub>2</sub> TCHP ( <b>Pd-5</b> )	$1.03 \times 10^4$	$2.06 \times 10^2$	$1.01 \times 10^4$

<sup>a</sup>  $k_{\text{r}}$ , radiative decay rate constant, calculated as  $k_{\text{r}} = \phi_{\text{phos}}k$ , where  $\phi_{\text{phos}}$  is the phosphorescence quantum yield.

<sup>b</sup>  $k_{\text{nr}}$ , nonradiative decay rate constant ( $k_{\text{nr}} = k_{\text{IC}} + k_{\text{ISC}}$ ), calculated as  $k_{\text{r}} = k - k_{\text{nr}}$ .